

Cuni-Sanchez, A., Sullivan, M. J. P., Platts, P. J., Lewis, S. L., Marchant, R., Imani, G., Hubau, W., Abiem, I., Adhikari, H., Albrecht, T., Altman, J., Amani, C., Aneseyee, A. B., Avitabile, V., Banin, L., Batumike, R., Bauters, M., Beeckman, H., Begne, S. K., Bennett, A. C., Bitariho, R., Boeckx, P., Bogaert, J., Bräuning, A., Bulonvu, F., Burgess, N. D., Calders, K., Chapman, C., Chapman, H., Comiskey, J., de Haulleville, T., Decuyper, M., DeVries, B., Dolezal, J., Droissart, V., Ewango, C., Feyera, S., Gebrekirstos, A., Gereau, R., Gilpin, M., Hakizimana, D., Hall, J., Hamilton, A., Hardy, O., Hart, T., Heiskanen, J., Hemp, A., Herold, M., Hiltner, U., Horak, D., Kamdem, M.-N., Kayijamahe, C., Kenfack, D., Kinyanjui, M. J., Klein, J., Lisingo, J., Lovett, J., Lung, M., Makana, J.-R., Malhi, Y., Marshall, A., Martin, E. H., Mitchard, E. T. A., Morel, A., Mukendi, J. T., Muller, T., Nchu, F., Nyirambangutse, B., Okello, J., Peh, K.-S.-H., Pellikka, P., Phillips, O. L., Plumptre, A., Qie, L., Rovero, F., Sainge, M. N., Schmitt, C. B., Sedlacek, O., Ngute, A. S. K., Sheil, D., Sheleme, D., Simegn, T. Y., Simo-Droissart, M., Sonké, B., Soromessa, T., Sunderland, T., Svoboda, M., Taedoumg, H., Taplin, J., Taylor, D., Thomas, S. C., Timberlake, J., Tuagben, D., Umunay, P., Uzabaho, E., Verbeeck, H., Vleminckx, J., Wallin, G., Wheeler, C., Willcock, S., Woods, J. T., Zibera, E. (2021): High aboveground carbon stock of African tropical montane forests. - Nature, 596, 536-542.

<https://doi.org/10.1038/s41586-021-03728-4>

High above-ground carbon stock of African tropical montane forests

Aida Cuni-Sanchez^{1,2*}, Martin J.P. Sullivan^{3,4}, Phil J. Platts^{1,5}, Simon L. Lewis^{4,6}, Rob Marchant¹, Gérard Imani⁷, Wannes Hubau^{8,9}, Iveren Abiem^{10,11}, Hari Adhikari¹², Tomas Albrecht^{13,14}, Jan Altman¹⁵, Christian Amani⁷, Abreham B. Aneseyee^{16,17}, Valerio Avitabile¹⁸, Lindsay Banin¹⁹, Rodrigue Batumike²⁰, Marijn Bauters²¹, Hans Beeckman⁸, Serge K. Begne^{4,22}, Amy C. Bennett⁴, Robert Bitariho²³, Pascal Boeckx²¹, Jan Bogaert²⁴, Achim Bräuning²⁵, Franklin Bulonvu²⁶, Neil D. Burgess²⁷, Kim Calders²⁸, Colin Chapman²⁹⁻³¹, Hazel Chapman^{11,33}, James Comiskey³⁴, Thales de Haulleville³⁵, Mathieu Decuyper^{36,37}, Ben DeVries³⁸, Jiri Dolezal^{15,39}, Vincent Droissart^{22,40}, Corneille Ewango⁴¹, Senbeta Feyera⁴², Aster Gebrekirstos⁴³, Roy Gereau⁴⁴, Martin Gilpin⁴, Dismas Hakizimana⁴⁵, Jefferson Hall⁴⁶, Alan Hamilton⁴⁷, Olivier Hardy⁴⁸, Terese Hart⁴⁹, Janne Heiskanen^{12,50}, Andreas Hemp⁵¹, Martin Herold^{37,52}, Ulrike Hiltner^{25,53}, David Horak⁵⁴, Marie-Noel Kamdem²², Charles Kayijamahe⁵⁵, David Kenfack⁴⁶, Mwangi J. Kinyanjui⁵⁶, Julia Klein⁵⁷, Janvier Lisingo⁴¹, Jon Lovett⁴, Mark Lung⁵⁸, Jean-Remy Makana⁵⁹, Yadvinder Malhi⁶⁰, Andrew Marshall^{1,61,62}, Emanuel H. Martin⁶³, Edward T.A. Mitchard⁶⁴, Alexandra Morel⁶⁵, John T. Mukendi⁸, Tom Muller⁶⁶, Felix Nchu⁶⁷, Brigitte Nyirambangutse^{68,69}, Joseph Okello^{21,70,71}, Kelvin S.-H. Peh^{72,73}, Petri Pellikka^{12,74}, Oliver L. Phillips⁴, Andrew Plumptre⁷⁵, Lan Qie⁷⁶, Francesco Rovero^{77,78}, Moses N. Sainge⁷⁹, Christine B. Schmitt^{80,81}, Ondrej Sedlacek⁵⁴, Alain S.K. Ngute^{61,82}, Douglas Sheil⁸³, Demisse Sheleme⁸⁴, Tibebu Y. Simegn⁸⁵, Murielle Simo-Droissart²², Bonaventure Sonké²², Teshome Soromessa¹⁶, Terry Sunderland^{86,87}, Miroslav Svoboda⁸⁸, Hermann Taedoumg^{89,90}, James Taplin⁹¹, David Taylor⁹², Sean C. Thomas⁹³, Jonathan Timberlake⁹⁴, Darlington Tuagben⁹⁵, Peter Umunay⁹⁶, Eustrate Uzabaho⁵⁵, Hans Verbeeck²⁸, Jason Vleminckx⁹⁷, Göran Wallin⁶⁹, Charlotte Wheeler⁶⁴, Simon Willcock^{98,99}, John T. Woods¹⁰⁰, Etienne Zibera⁶⁸

Abstract

Tropical forests store 40-50% of terrestrial vegetation carbon¹. Spatial variations in aboveground live tree biomass carbon (AGC) stocks remain poorly understood, in particular in tropical montane forests². Owing to climatic and soil changes with increasing elevation³, AGC stocks are lower in tropical montane compared to lowland forests². Here we assemble and analyse a dataset of structurally intact old-growth forests (AfriMont) spanning 44 montane sites in 12 African countries. We find that montane sites in the AfriMont plot network have a mean AGC-stock of 149.4 Mg C ha⁻¹ (95% CI 137.1-164.2), comparable to lowland forests in the African Tropical Rainforest Observation Network⁴ and about 70 per cent and 32 per cent higher than averages from plot networks in montane^{2,5,6} and lowland⁷ forests in the Neotropics, respectively. Notably, our results are two-thirds higher than the IPCC default values for these forests in Africa⁸. We find that the low stem density and high abundance of large trees of African lowland forests⁴ is mirrored in the montane forests sampled. This carbon store is endangered: we estimate that 0.8 million ha of old-growth African montane forest have been lost since 2000. We provide country-specific montane forest AGC stock estimates modelled from our plot network to help guide forest conservation and reforestation interventions. Our findings highlight the need for conserving these biodiverse^{9,10} and carbon-rich ecosystems.

43 **Main text**

44 Tropical forests cover less than 10% of the global land area yet store 40–50% of terrestrial
45 vegetation carbon¹ and contribute more than one third of primary productivity¹¹ so are a key
46 component of the global carbon cycle^{12,13}. There is substantial variation in carbon stocks across the
47 biome, with lowland forests in Africa and Borneo storing more carbon per unit area than lowland
48 forests in the Neotropics^{4,7}. This variation arises partly from structural differences: the signature
49 feature of African forests is their low stem density but relatively high abundance of large trees (>70
50 cm diameter) which store large quantities of carbon, while Bornean forests are characterised by high
51 stem density and basal area^{4,14,15}.

52

53 Despite increased understanding of biogeographic differences in tropical lowland forests, patterns of
54 spatial variation in carbon stocks remain poorly understood in the 880,000 km² of tropical montane
55 forests located $\geq 1,000$ m asl². Montane forests are expected *a priori* to have lower aboveground live
56 tree biomass carbon (AGC) stocks than lowland forests because (1) temperature decreases with
57 increasing elevation, reducing net primary productivity and slowing nutrient recycling, (2) long
58 periods of cloud immersion in montane forests suppresses productivity, (3) soil waterlogging slows
59 nutrient recycling and (4) high epiphyte load, local wind exposure in crests and nutrient-limited soils
60 limit tree size and increase investment in roots over shoots³. While forest inventory plots provide
61 some support for these assumptions² data from African mountain regions are exceptionally sparse.
62 Indeed, in the most recent IPCC guidelines, there is no specific AGC default value for old-growth
63 montane forests in Africa: the value given of 89.3 Mg C ha⁻¹ is simply a mean of secondary and old-
64 growth forests found $\geq 1,000$ m asl⁸. Mountain areas also pose special challenges for remote-sensing
65 approaches for estimating carbon stocks, as radar data are affected by geometric distortions¹⁶ while
66 steep slopes bias spaceborne LiDAR estimates towards overestimating canopy height¹⁷. These issues
67 are reflected in the limited correlation between estimates of AGC-stocks at mountain locations from
68 different recent remote-sensing derived carbon maps (Supplementary Information Table S1).

69

70 Better understanding of montane carbon stocks is important for many African countries, particularly
71 in eastern Africa where montane forests represent most of the extant evergreen old-growth forest
72 cover. Quantifying carbon stocks in these ecosystems is critical for estimating national carbon losses
73 from deforestation and forest degradation¹⁸. Quantifying carbon stocks in old-growth montane
74 forests also serves to constrain potential carbon uptake by restored natural forests, given the high
75 commitment of most African nations to the Bonn Challenge effort to restore 150 million ha of
76 degraded and deforested lands by 2020 (see Table 1), and 350 million by 2030.

77

78 Here we measured, compiled and analysed a new dataset of 226 plot inventories spanning 44 sites
79 in 12 African countries, covering most major mountain regions on the continent (the “AfriMont”
80 dataset). Plots range from 800 to 3,900 m asl to include submontane forests (800-1,000 m asl) in
81 smaller mountains closer to the ocean^{19,20}. For all plots, stem diameter and species were recorded
82 for each tree ≥ 10 cm diameter at breast height (or above buttress) following standard methods²¹.
83 Tree height was sampled in 23 montane sites, allowing variation in height-diameter allometry to be
84 incorporated into the calculation of aboveground biomass. A total of 72,336 stems with diameter
85 ≥ 10 cm were measured. For each tree, we computed AGC (in Mg C ha⁻¹) according to standard
86 procedures (see methods).

87

88 We find that the mean plot-level AGC-stock across sampled African tropical montane forests is 149.4
89 Mg C ha⁻¹ (95% confidence interval (CI) 137.1-164.2), two-thirds more than the IPCC default value of
90 89.3 Mg C ha⁻¹. Our estimates are robust to subsampling our dataset (Extended Data Fig. 1) and
91 excluding small plots (Extended Data Fig. 2) and are not affected by the sampling strategy used to
92 establish plots in each study site (Extended Data Fig. 2). Comparing our dataset to previous
93 syntheses of montane^{2,5,6} and lowland⁷ forest plot networks reveals that tropical montane forests in

94 Africa have significantly higher AGC-stocks per unit area than both montane (95% CI = 50.4 – 71.9
95 Mg C ha⁻¹) and lowland (95% CI = 124.0 – 147.9 Mg C ha⁻¹) forests in the Neotropics, and that they
96 do not differ significantly from lowland forests in Africa (95% CI = -27.6 – 9.6 Mg C ha⁻¹) (Fig. 1, Table
97 S2). The similar AGC-stocks in montane and lowland forests in Africa contrasts with the Neotropics
98 and Southeast Asia, where carbon stocks are lower in montane forests than lowland forests (albeit
99 not significantly different in Southeast Asia due to the small sample size, Fig. 1). These differences
100 are robust to accounting for differences in elevation among montane datasets: removing African
101 plots 800-1,000 m asl slightly reduces estimated montane forest AGC-stock to 145.0 Mg C ha⁻¹ (95%
102 CI 129.6 – 163.2), but observed differences in AGC-stock among continents remain when plots are
103 restricted to elevations well represented in all continents (Extended Data Fig. 3).

104

105 The characteristic structural properties of lowland African forests (relatively low stem density and
106 greater importance of large trees compared to elsewhere in the tropics⁴) are also evident in the
107 African montane forests we sampled. In these montane forests mean stem density is 483.3 stems ha⁻¹
108 (± 177.7 s.d.) and mean basal area is 39 m²ha⁻¹ (± 14.8 s.d.). We find a high density of large stems
109 (>70 cm diameter, 19.1 stems ha⁻¹ ± 15.4 s.d.) which contribute 35.3% (95% CI = 29.6 – 41.8 %) to
110 plot-level AGC-stock (Fig. 2). The contribution of large trees to plot-level AGC-stock is also similar in
111 montane and lowland Africa (95% CI of difference in square-root transformed proportional
112 contribution of large trees between lowland and montane forests = -0.100 - 0.075, $P = 0.80$). There
113 was no significant difference in the proportional contribution of any other size class to AGC-stocks
114 between our montane dataset and 132 lowland plots from the AfriTRON network ($P \geq 0.24$, Table S3),
115 although greater variation among plots is observed in montane forests (Fig. 2).

116

117 To investigate if elevation affected AGC or forest structure, we modelled these variables as functions
118 of elevation using random slopes mixed-effects models. This approach allows intercepts and
119 relationships to vary among sites, which would be expected as mountains can have very different
120 climate at the same elevation due to proximity to the ocean (generally the further, the drier) and
121 because of the mass-elevation or telescopic effect²² (larger mountains are better at warming the
122 atmosphere above them). We found that AGC, stem density or density of large stems (>70 cm
123 diameter) were not significantly related to elevation (Fig. 3, Table S4). Across sites these non-
124 significant relationships were all negative, although there was some variation in strength and
125 direction amongst sites (Fig. 3). Similarly, in the Neotropics and Southeast Asia montane forest plot
126 datasets, AGC was not significantly correlated with elevation (Extended Data Fig. 4).

127

128 To assess potential environmental drivers of AGC-stock variation across the AfriMont plot network,
129 we related AGC to climate, soil and topography. We found that AGC-stocks increased with annual
130 precipitation (albeit not statistically significantly), decreased with soil fertility and were higher in
131 plots which were locally at higher elevation than their surroundings (Extended Data Fig. 5).
132 Relationships with other environmental variables were non-significant (Extended Data Fig. 5).
133 Although global datasets might not capture fine-scale variation in climate or soils in mountain
134 regions²³, leading to regression dilution²⁴, the general absence of strong climate effects combined
135 with the lack of significant effect of elevation on AGC-stocks suggest that the high AGC-stock of
136 African montane forests is a pervasive phenomenon across a wide environmental gradient.

137

138 Although the AfriMont dataset covers most major mountain areas in tropical Africa (Fig. 4), some
139 areas remain under-sampled relative to forest extents (Extended Data Fig. 6), resulting in some
140 differences between the environmental conditions sampled by our plot network and the wider
141 montane forest biome in Africa (Extended Data Fig. 7). Notably, the absence of plots from montane
142 forests of eastern Democratic Republic of the Congo (Fig. 4, Extended Data Fig. 6) means that the
143 AfriMont dataset samples forests are, on average, at higher elevations, and that are cooler and
144 cloudier than the wider montane forest biome in Africa (Extended Data Fig. 7). Using relationships

145 with environmental variables (Extended Data Fig. 5) to predict AGC-stocks in each 1-km grid cell
146 containing montane forest gives a mean (weighted by remaining forest cover) AGC-stock of 176.9
147 Mg C ha⁻¹ (\pm 32.0 s.d.) for the tropical montane forest biome in Africa. This indicates that the
148 estimate we report based on our AfriMont plot network data (149.4 Mg C ha⁻¹) is conservative.

149
150 Several mechanisms could explain the high AGC-stock of montane forests in the AfriMont plot
151 network. Firstly, large herbivores such as elephants (*Loxodonta* spp.) can have profound effects on
152 forest structure by consuming biomass, destroying small stems, dispersing seeds and transporting
153 nutrients²⁵. Studies for lowland forests suggest that elephants can increase carbon stocks^{26,27}. We
154 tested if AfriMont plots with known elephant presence as of 2019 had significantly higher AGC-
155 stocks, but found that they had significantly lower AGC-stocks, although significant differences were
156 not observed in some countries (Extended Data Fig. 8). While the initial ecosystem response to
157 elephant removal might be greater AGC-stocks due to reduced biomass consumption and small-stem
158 destruction, the longer-term effects might differ. We were unable to fully disentangle such effects,
159 as we lacked details on both i) time since elephant extirpation, and ii) elephant abundance and its
160 determinants (see Table S5).

161
162 A second potential explanation is a relatively low frequency of large-scale abiotic disturbances,
163 allowing trees time to grow large and stands to self-thin, as is seen in lowland African forests⁴. For
164 example, tropical cyclones are largely absent in mainland Africa (except in Mozambique²⁸) and lava
165 flows are limited even in the active volcano of Mt Cameroon²⁹. Although fine-scale variability in
166 landslide risk limits comparisons across large spatial scales, there are fewer areas with high landslide
167 susceptibility in mountains in tropical Africa than in the Andes and most mountain ranges in
168 Southeast Asia³⁰. If forests have been ecologically stable over evolutionary timescales, tree species
169 may be adapted to grow slowly but potentially reaching great sizes³¹. On Mt Kilimanjaro
170 *Entandrophragma* individuals reach enormous heights and ages³². This low frequency of large-scale
171 abiotic disturbances contrasts with the Andes and several mountains in Southeast Asia (e.g. Barisan
172 mountains in western Sumatra), which are tectonically active, so the trees there are adapted to
173 sudden disturbance followed by intense competition to get established and grow. Future monitoring
174 of the AfriMont plot network will help determine the extent to which the high biomass of African
175 tropical montane forests results from them being dynamic and productive, or adapted to stability.

176
177 A third potential explanation could be the presence of conifers³³. Mixed conifer/broad-leaved forests
178 tend to have greater basal area than purely broad-leaved forests due to a more effective use of light
179 and other resources³⁴. Podocarpaceae can be found in montane forests across the tropics³⁵. Despite
180 having fewer species in Africa than in other continents³⁶, these could be more abundant at the site-
181 level. However, there is no pantropical comparative study on Podocarpaceae abundance in tropical
182 montane forests. In our dataset there was no significant correlation between plot-level AGC-stock
183 and conifer (Podocarpaceae) abundance (Extended Data Fig. 9). Other explanations could be
184 continental differences in mountain terrain (more gentle slopes or plateau regions in Africa) or types
185 of montane forests investigated (less cloud forest existing/sampled in Africa). Within our dataset,
186 slope did not have a significant effect on AGC-stocks (Extended Data Fig. 5). Contrary to the
187 Neotropics³⁷, there is no high-resolution map of cloud forests available for Africa, so while we found
188 no relationship between AGC-stock and cloud frequency (Extended Data Fig. 5), we were unable to
189 investigate differences in AGC-stock between cloud forest vs non-cloud forest plots.

190
191 To understand the policy implications of our findings for African countries, we calculated montane
192 (\geq 800 m asl) forest cover change between 2000 and 2018, using forest cover from ref.³⁸ clipped to
193 'primary humid forest' from ref.³⁹. We show that tropical montane forests represent most -or all-
194 evergreen old-growth forests found in ten African countries (Fig. 4), and that the Democratic
195 Republic of the Congo has two thirds of the remaining 16 million ha of montane forests in Africa.

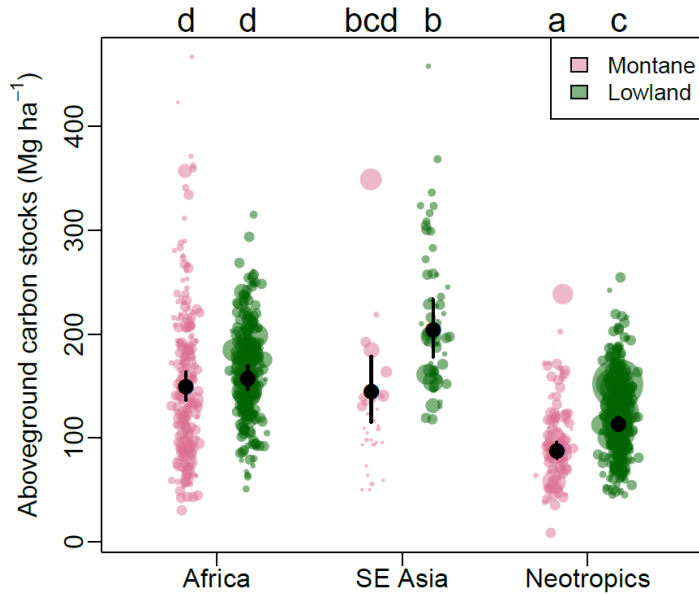
196 Over 0.8 million ha (5%) have been lost in Africa since 2001, with the highest losses in the
197 Democratic Republic of the Congo (536,000 ha), Uganda (65,000 ha) and Ethiopia (62,000 ha) (Fig. 4,
198 Table 1). In terms of percentage, Mozambique and Côte d'Ivoire lost over 20% of their montane
199 forests over this period (Fig. 4, Table 1). In some sites, however, a larger proportion of montane
200 forests was lost before 2000, e.g. in Taita Hills in Kenya⁴⁰. If absolute country-level deforestation
201 rates continue, a further 0.5 million ha of tropical montane forests will be lost by 2030.

202
203 African tropical montane forests are not only carbon-rich, but they also harbour some of the highest
204 concentrations of biodiversity and endemism in the world^{9,10}. They are important 'water towers' as,
205 located at the headwaters of numerous river systems, including the Congo and the Nile, they
206 regulate timing and magnitude of runoff⁹. They also regulate local temperatures⁴¹ and provide
207 numerous other services to people in the surrounding landscapes⁹. Clearly, more should be done to
208 avoid the destruction of these important ecosystems. Logging, mining and clearing land for farming,
209 but also political unrest and militia presence have affected -and continue to affect- these forests, e.g.
210 in Itombwe Mts in the Democratic Republic of the Congo⁴². Protected areas are known to help
211 reduce deforestation in the tropics⁴³. Beyond protected areas, other forest conservation
212 mechanisms could be implemented, including effective carbon finance. Previous IPCC AGC-stock
213 estimates for montane forests in Africa (89.3 Mg C ha⁻¹) may have contributed to low incentives for
214 carbon finance mechanisms in these ecosystems. Our study shows the far greater carbon storage
215 potential in these tropical montane forests, which will be even higher if soil carbon stocks are
216 considered (e.g. > 200 Mg C ha⁻¹ of organic carbon occurs in the top 0-30 cm soil on Mt Cameroon⁴⁴
217 and in the Usambara Mts, Tanzania⁴⁵).

218
219 As well as conserving the remaining montane forests, efforts to restore them are critical. Forest
220 restoration at one of our sites, Kibale National Park in Uganda, indicates the potential for rapid AGC
221 accumulation⁴⁶. Our study shows the high potential AGC-stock these montane forests can attain. The
222 possible co-benefits of forest restoration, notably water regulation, control of soil erosion and
223 landslides and biodiversity conservation should also be considered. Most African nations are
224 committed to the Bonn Challenge; Ethiopia leading with 15 million ha committed (Table 1). We
225 provide country-specific estimates of potential AGC-stocks based on forests sampled in the AfriMont
226 dataset to help guide such interventions (Table 1, Extended Data Fig. 10). Caution is needed when
227 scaling-up our estimates to the landscape scale, as not all forests are closed-canopy old-growth and
228 structurally intact. Remote sensing or ancillary data (landcover maps, spatial environmental data)
229 could be used to identify e.g. exotic plantations, degraded or bamboo forests, and thus help create
230 detailed AGC maps at different spatial scales^{18,47}. A closer collaboration between air-borne, space-
231 borne and ground approaches (such as the AfriMont and AfriTRON plot networks) is key for accurate
232 quantification and monitoring of landscape-scale tropical forest AGC-stocks, particularly in mountain
233 regions.

234
235 Our newly compiled dataset and analysis provides a large-scale quantification of AGC-stock in
236 African tropical montane forests, indicating it to be on average substantially higher than previously
237 thought. While there is variation around this mean AGC-stock within and across sites, it is not
238 systematically related to elevation. Apart from helping refine country-level estimates, IPCC
239 guidelines and ground-calibration of remote-sensing estimates, continued on-the-ground monitoring
240 of the AfriMont plot network will help determine ecosystem dynamics and carbon residence time in
241 these extraordinarily carbon-rich forests, as well as their responses to climatic changes.

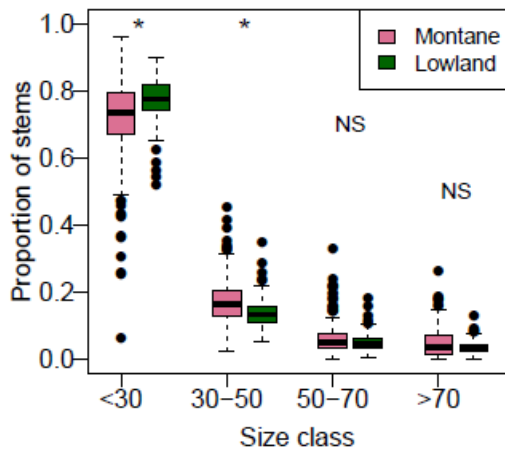
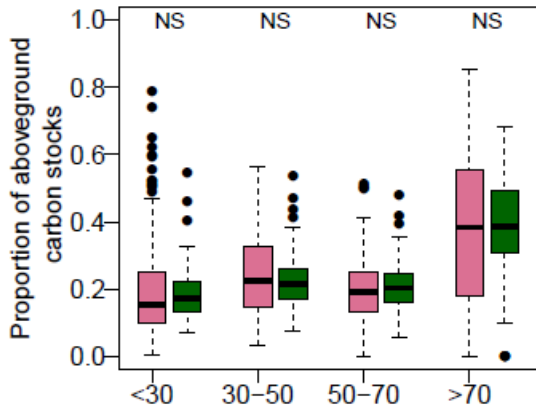
242
243



245
246

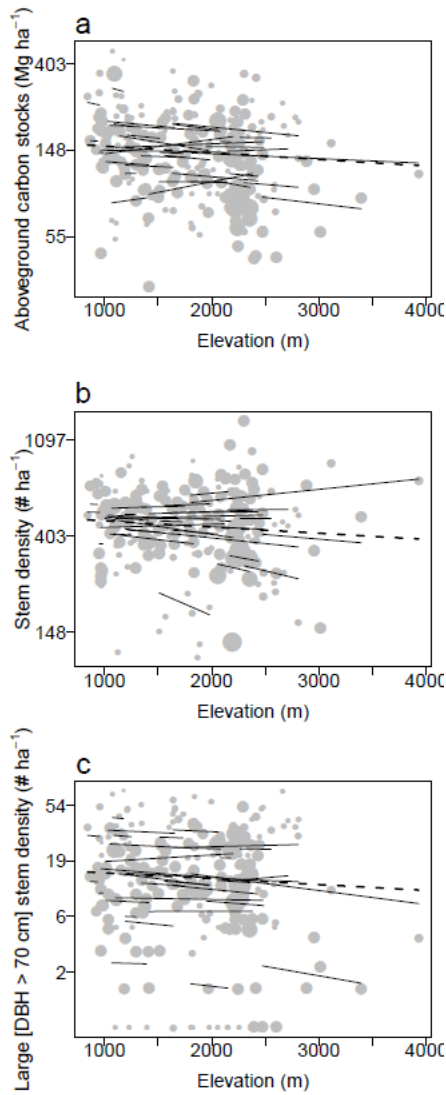
247 **Fig. 1 | Pantropical variation in aboveground carbon stocks sampled by plot networks in montane**
 248 **(≥ 800 m asl) and lowland (< 800 m asl) tropical forests.** Data from this study for African montane
 249 forests ($n = 226$ plots, this study), montane forests in the Neotropics ($n = 131$) and Southeast Asia (n
 250 $= 32$) are from ref.^{2,5,6}, lowland forests in Africa ($n = 290$), the Neotropics ($n = 416$) and Southeast
 251 Asia ($n = 60$) are from ref.⁷. Coloured points show the AGC-stock in each plot, with point size
 252 proportional to square-root plot area. Black points show means for each continent-elevation
 253 category estimated using linear mixed-effects models with site as a random effect, and lines show
 254 95% confidence intervals around means. Letters indicate significant differences between continent
 255 elevation category combinations (linear mixed-effects models with site as a random effect, $P < 0.05$).

256
257



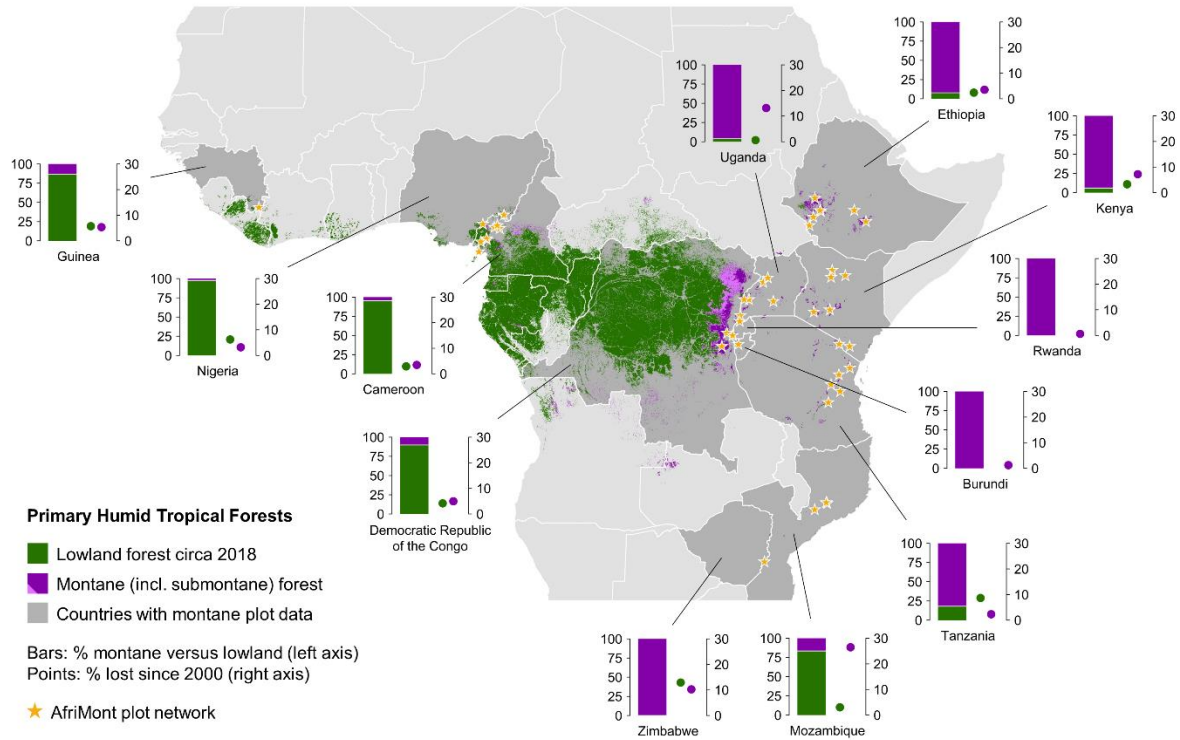
258
 259
 260
 261
 262
 263
 264
 265
 266

Fig. 2 | Proportion of plot-level aboveground carbon stock and stems accounted for by each size class in montane and in lowland forests in Africa. Statistically significant differences in contribution of each size class between montane and lowland forest plot networks are shown by asterisks (linear mixed-effects model, $P < 0.05$). NS = non-significant difference. Montane ($n = 226$), lowland ($n = 132$). The thick line shows the median, and boxes cover the interquartile range (IQR). Values > 1.5 times IQR away from the IQR are shown by points.



267
 268
 269
 270
 271
 272
 273
 274
 275
 276
 277
 278
 279

Fig. 3 | Variables as a function of elevation. a-c Relationship between elevation and plot-level AGC stock (a), stem density (b) and stem density of large stems (>70 cm diameter; c) for the AfriMont dataset. Note log-scale of y-axis. Each response variable was log-transformed and modelled as a function of elevation with a linear mixed-effect models with random slopes. The dashed line shows the relationship across sites (non-significant in all cases, $P \geq 0.3$, Table S4), while the black lines show the relationship within each site. Point sizes are proportional to square-root plot area. A polynomial model allowing a non-linear relationship with elevation was also tested but not supported over the linear model in any case ($P \geq 0.7$, Table S4). The absence of a significant relationship with elevation is robust to removing the two highest elevation sites, Rwenzori and Virunga (Table S4). DBH diameter at breast height.



280
 281
 282
 283
 284
 285
 286
 287

Fig. 4. | Old-growth evergreen humid forests in lowland and montane tropical Africa. Forest extends circa 2018. Note that montane includes submontane forests (800-1,000 m asl, light purple). Montane forests represent most (or all) evergreen humid old-growth forest in ten African nations: Burundi, Ethiopia, Kenya, Rwanda, Tanzania, Uganda and Zimbabwe (included in AfriMont); and Zambia, Malawi and South Sudan (no plot data available). Forest cover extracted from ref.³⁸ and clipped to 'primary humid forest' using ref.³⁹. See Table 1 for country-level absolute estimates.

288 **Table 1 | Remaining forest area and aboveground carbon estimates for montane and lowland**
 289 **tropical forests in Africa**
 290

Country	Montane (ha)	Montane lost (ha)	Montane AGC (MgC ha ⁻¹ , 95% CI)	Montane sites (plots)	Lowland (ha)	Lowland AGC (MgC ha ⁻¹ , 95% CI)	Lowland plots	Bonn Challenge by 2020 (ha)
Burundi	25,000	300	94 (47-176)	1 (7)	0		0	2 million
Cameroon	840,000	30,200	153 (121-195)	7 (37)	17.7 million	166 (151-185)	72	12 million
DRC	10.2 million	536,500	129 (84-202)	2 (37)	90 million	158 (135-183)	48	8 million
Ethiopia	1.7 million	62,100	165 (124-215)	8 (25)	145,000	^a	0	15 million
Guinea	29,000	1,700	314 (147-616) ^b	1 (2)	193,000	157 (122 – 206) ^c	24	2 million
Kenya	568,000	44,100	104 (79-136)	8 (38)	37,000		0	5.1 million
Mozambique	18,000	6,600 ^d	226 (146-384) ^b	3 (4)	93,000	^e	0	1 million
Nigeria	42,000	1,400	120 (47-309) ^b	1 (1)	1.8 million	161 (105-262)	2	4 million
Rwanda	53,000	300	106 (65-168)	2 (11)	0		0	2 million
Tanzania	587,000	13,900	175 (129-234)	6 (29)	130,000	128 (101-163)	16	5.2 million
Uganda	427,000	64,600 ^d	158 (111-209)	6 (23)	18,000		0	2.5 million
Zimbabwe	7,000	800 ^d	203 (108-363)	1 (12)	<1,000		0	2 million

291

292 Forest cover circa 2018 was extracted from ref.³⁸ and clipped to 'primary humid forest' using ref.³⁹.
 293 Montane forest lost covers the period 2000-2018. Mean aboveground carbon (AGC, in MgC ha⁻¹)
 294 estimates for montane (or lowland) forests were estimated from AfriMont and AfriTRON plot
 295 network data. Mean AGC values are in boldface, 95% confidence intervals in parentheses. For details
 296 on sites and plots used see Table S5. Bonn Challenge pledges for 2030 not yet available.

297 ^a Ref.⁴⁸ report 192 MgC ha⁻¹ for lowland.

298 ^b Few plots sampled, or very small plots sampled, AGC estimates may not be robust, see Extended
 299 data Fig. 10.

300 ^c Data from neighbouring Liberia.

301 ^dMontane forest loss in Mozambique, Uganda and Zimbabwe represents 27%, 13% and 10% of the
 302 existing montane forest in 2001, respectively. Montane forest loss in Côte d'Ivoire (no plot data
 303 available) was estimated to be 21% for the same period.

304 ^e Ref.⁴⁹ report 132.2 MgC ha⁻¹ for lowland.

305

306

307 **References**

- 308 1. Erb, K., et al. Unexpectedly large impact of forest management and grazing on global
 309 vegetation biomass. *Nature* **553**, 73–76 (2018).
- 310 2. Spracklen, D.V. & Righelato, R. Tropical montane forests are a larger than expected global
 311 carbon store. *Biogeosciences* **11**, 2741–2754 (2014).
- 312 3. Fahey, T. J., Sherman, R. E. & Tanne, E. V. J. Tropical montane cloud forest: environmental
 313 drivers of vegetation structure and ecosystem function. *J. Trop. Ecol.* **32**, 355–367 (2016).
- 314 4. Lewis, S. L. et al. Above-ground biomass and structure of 260 African tropical forests. *Phil.*
 315 *Trans. R. Soc. Lond. B* **368**, 20120295 (2013).
- 316 5. Vilanova, E. et al. Environmental drivers of forest structure and stem turnover across
 317 Venezuelan tropical forests. *PLoS ONE* **13**(6): e0198489 (2018).
- 318 6. Alvarez-Davila, E. et al. Forest biomass density across large climate gradients in northern
 319 South America is related to water availability but not with temperature. *PLoS ONE* **12**(3):
 320 e0171072 (2017).
- 321 7. Sullivan, M. J. P., et al. Long-term thermal sensitivity of Earth’s tropical forests. *Science* **368**,
 322 869–874 (2020).
- 323 8. Domke, G. et al. in 2019 Refinement to the 2006 IPCC Guidelines for National Greenhouse
 324 Gas Inventories Vol. 4 (eds Calvo Buendia, E. et al.) Ch. 4, 48 (IPCC, 2019).
- 325 9. *African Mountains Atlas* (UNEP, 2014).
- 326 10. Rahbek, C., et al. Humboldt’s enigma: What causes global patterns of mountain biodiversity?
 327 *Science* **365**, 1108–1113 (2019).
- 328 11. Pan, Y. et al. A large and persistent carbon sink in the world’s forests. *Science* **333**, 988–993
 329 (2011).
- 330 12. Booth, B. B. B. et al. High sensitivity of future global warming to land carbon cycle processes.
 331 *Environ. Res. Lett.* **7**, 024002 (2012).
- 332 13. Hubau, W., et al. Asynchronous carbon sink saturation in African and Amazonian tropical
 333 forests. *Nature* **579**, 80–87 (2020).
- 334 14. Feldpausch, T. R. et al. Tree height integrated into pantropical forest biomass estimates.
 335 *Biogeosciences* **9**, 3381–3403 (2012).
- 336 15. Bastin, J.-F., et al. Pan-tropical prediction of forest structure from the largest trees. *Global*
 337 *Ecol. Biogeogr.* **27**, 1366–1383 (2018).
- 338 16. CCI BIOMASS Product User Guide Year 1 Version 1.0. (Aberystwyth University and GAMMA
 339 Remote Sensing, 2019)
 340 https://climate.esa.int/sites/default/files/biomass_D4.3_Product_User_Guide_V1.0.pdf
- 341 17. Lefsky, M. A., Keller, M., Pang, Y., de Camargo, P. & Hunter, M. O. Revised method for forest
 342 canopy height estimation from the Geoscience Laser Altimeter System waveforms. *J. Appl.*
 343 *Remote Sens.* **1**, 013537 (2007).
- 344 18. Willcock, S., et al. Quantifying and understanding carbon storage and sequestration within
 345 the Eastern Arc Mountains of Tanzania, a tropical biodiversity hotspot. *Carbon Balance*
 346 *Manage.* **9**, 2 (2014).
- 347 19. Bussmann, R.W. Vegetation zonation and nomenclature of African Mountains – An
 348 overview. *Lyonia* **11**, 41–66 (2006).
- 349 20. Hamilton, A. Vegetation, climate and soil, altitudinal relationships on the East Usambara
 350 Mountains of Tanzania. *J. E. Afr. Nat. Hist.* **87**, 1-5 (1998).
- 351 21. Phillips, O., Baker, T., Brienen, R. & Feldpausch, T. RAINFOR field manual for plot
 352 establishment and remeasurement.
 353 http://www.rainfor.org/upload/ManualsEnglish/RAINFOR_field_manual_version_2016.pdf
 354 (Univ. Leeds, 2016).
- 355 22. Jarvis, A. & Mulligan, M., The climate of cloud forests. *Hydrol. Process.* **25**, 327–343 (2011).
- 356 23. Platts, P.J., Omeny, P.A. & Marchant, R. AFRICLIM: high-resolution climate projections for
 357 ecological applications in Africa. *Afr. J. Ecol.* **53**, 103–108 (2015).

- 358 24. McInerney, G. J., Purves, D. W. Fine-scale environmental variation in species distribution
359 modelling: Regression dilution, latent variables and neighbourly advice. *Methods Ecol. Evol.*
360 **2**, 248–257 (2011).
- 361 25. Poulsen, J.R., et al. Ecological consequences of forest elephant declines for Afrotropical
362 forests. *Conserv. Biol.* **32**, 559–567 (2018).
- 363 26. Berzaghi, F., et al. Carbon stocks in central African forests enhanced by elephant
364 disturbance. *Nat. Geosci.* **12**, 725–729 (2019).
- 365 27. Enquist, B.J., et al. The megabiota are disproportionately important for biosphere
366 functioning. *Nat. Commun.* **11**, 699 (2020).
- 367 28. Lin, T.-C., Hogan, J.A. & Chang, C.T. Tropical Cyclone Ecology: A Scale-Link Perspective.
368 *Trends Ecol. Evol.* **35**, 594–604 (2020).
- 369 29. Favalli, M., et al. Lava flow hazard and risk at Mt. Cameroon volcano. *Bull. Volcanol.* **74**, 423–
370 439 (2012).
- 371 30. Stanley, T. & Kirschbaum, D.B. A heuristic approach to global landslide susceptibility
372 mapping. *Nat. Hazards* **87**, 145–164 (2017).
- 373 31. Lovett, J. C. Elevational and latitudinal changes in tree associations and diversity in the
374 Eastern Arc mountains of Tanzania. *J. Trop. Ecol.* **12**, 629–650 (1996).
- 375 32. Hemp, A., et al. Africa’s highest mountain harbours Africa’s tallest trees. *Biodiv. Conserv.* **26**,
376 103–113 (2016).
- 377 33. Culmsee, H., Leuschner, C., Moser, G. & Pitopang, R., Forest aboveground biomass along an
378 elevational transect in Sulawesi, Indonesia, and the role of Fagaceae in tropical montane rain
379 forests. *J. Biogeogr.* **37**, 960–974 (2010).
- 380 34. Enright, N.J. & Ogden, J. The southern conifers - a synthesis. Ecology of the southern conifers
381 (ed. by N.J. Enright & Hill R.S.), pp. 271–287. Melbourne University Press, Melbourne (1995).
- 382 35. Neale, D. B. & Wheeler, N. C. The Conifers. In: The Conifers: Genomes, Variation and
383 Evolution (eds. Neale, D. B. & Wheeler, N. C.) pp 1–21. Springer International Publishing
384 (2019).
- 385 36. Mill, R. R. Towards a Biogeography of the Podocarpaceae. In IV International Conifer
386 Conference, R. R. Mill, ed. *Acta Hort.* **615**, 137–147 (2003).
- 387 37. Helmer, E.H., Gerson, E.A., Baggett, L.S., Bird, B.J., Ruzycski, T.S. & Voggeser, S.M.
388 Neotropical cloud forests and paramo to contract and dry from declines in cloud immersion
389 and frost. *PLoS ONE* **14**(4): e0213155 (2019).
- 390 38. Hansen, M. C., et al. High-Resolution Global Maps of 21st-Century Forest Cover Change.
391 *Science* **342**, 850-853 (2013).
- 392 39. Turubanova, S., Potapov, P., Tyukavina, A. & Hansen M. Ongoing primary forest loss in Brazil,
393 Democratic Republic of the Congo, and Indonesia. *Environ. Res. Lett.* **13**, 074028 (2018).
- 394 40. Pellikka, P. K. E., Lötjönen, M., Siljander, M. & Lens, L. Airborne remote sensing of
395 spatiotemporal change (1955–2004) in indigenous and exotic forest cover in the Taita Hills,
396 Kenya. *Int. J. Appl. Earth Obs.* **11**, 221–232 (2009).
- 397 41. Zeng, Z. et al. Deforestation-induced warming over tropical mountain regions regulated by
398 elevation. *Nat. Geosci.* **14**, 23–29 (2020). <https://doi.org/10.1038/s41561-020-00666-0>
- 399 42. Spira, C., Kirkby, A., Kujirakwinja, D. & Plumptre, A. J. The socio-economics of artisanal
400 mining and bushmeat hunting around protected areas: Kahuzi– Biega National Park and
401 Itombwe nature reserve, eastern Democratic Republic of Congo. *Oryx* **53**, 136–144(2017).
- 402 43. Bebbler, D.P. & Butt, N. Tropical protected areas reduced deforestation carbon emissions by
403 one third from 2000-2012. *Sci. Rep.* **7**, 14005 (2017).
- 404 44. Tegha, K. C. & Sendze, Y. G., Soil organic carbon stocks in Mt Cameroon National Park under
405 different land uses. *J. Ecol. Nat. Environ.* **8**, 20–30, (2016).
- 406 45. Munishi, P.K.T. & Shear, T.H. Carbon storage in afro-montane rain forests of the eastern arc
407 mountains of Tanzania: their net contribution to atmospheric carbon. *J. Trop. For. Sci.* **16**,
408 78–98 (2004).

- 409 46. Wheeler, C.E., et al. Carbon sequestration and biodiversity following 18 years of active
410 tropical forest restoration. *Forest Ecol. Manage.* **373**, 44–55 (2016).
- 411 47. Avitabile, V., Baccini, A., Friedl, M.A. & Schmillius, C. Capabilities and limitations of Landsat
412 and land cover data for aboveground woody biomass estimation of Uganda. *Remote Sens.*
413 *Environ.* **117**, 366–380 (2012).
- 414 48. Aneseyee, B A., Soromessa, T. & Belliethathan, S. Carbon Sock of Gambella National Park:
415 Implication for Climate Change Mitigation. *Int. J. Adv. Life Sci.* **35**, 41–56 (2015).
- 416 49. Lisboa, S.N., et al. Biomass allometric equation and expansion factor for a mountain moist
417 evergreen forest in Mozambique. *Carbon Balance Manage.* **13**, 23 (2018).

418

419 **Methods**

420 **AfriMont or montane Africa dataset**

421 We compiled forest inventory plot data from the African Tropical Rainforest Observatory Network
422 (AfriTRON; www.afritron.org), with data curated at www.ForestPlots.net^{50,51} and the TEAM
423 network⁵², as well as from numerous site-specific publications detailed in Table S5 and mapped in
424 Fig. 4. Plots were selected for the analysis when conforming to the following criteria: ≥800 m asl,
425 closed-canopy evergreen wet or moist tropical forest, geo-referenced, old-growth and structurally
426 intact (not impacted by recent selective logging, fire or coffee cultivation), with no exotic species
427 present (e.g. *Eucalyptus* or *Pinus* spp.), all trees ≥10 cm diameter measured and majority of stems
428 identified to species. We included plots from Virunga Massif in Rwanda/Uganda even when not
429 100% closed-canopy due to high abundance of naturally-occurring bamboo. In all plots, tree
430 diameter was measured at 1.3 m along the stem from the ground, or above buttresses if present. In
431 23 sites tree height was sampled in the field for some stems, using a clinometer or a laser. Families
432 and species names follow the African Plant Database (<http://africanplantdatabase.ch>). The AfriMont
433 dataset consists of 72,336 stems, of which 92.9% were identified to species, 98.4% to genus and
434 98.5% to family. This dataset represents a standardised safe long-term repository of valuable
435 historical data (four sites initially considered could not be included because tree-level data had
436 already been lost by data owners).

437

438 **AfriTRON or lowland Africa dataset**

439 The 132 lowland-forest plots are all from AfriTRON^{4,13,53}. They were selected using the same criteria
440 as above (but with elevation <800 m asl), restricted to countries for which we also had montane
441 plots plus neighbouring countries where the mountains span international borders (e.g. Mt Nimba
442 spans Guinea and Liberia). The dataset includes 51,305 stems, of which 89.6% were identified to
443 species, 97.3% to genus and 97.7 % to family. The plot data were retrieved from forestplot.net on
444 06/01/2019. The plot locations and details are in Table S6.

445

446 **Literature dataset**

447 We compiled data on AGC-stocks in tropical lowland and montane forests to compare to the
448 AfriMont data. Data for lowland forests came from ref.⁷ and consisted of all multi- and single-census
449 plots that were <800 m asl. Data for montane forests were obtained from ref.², with additional data
450 from Venezuela (ref.⁵) and Colombia (ref.⁶). Montane plots were defined as ≥800 m asl; elevation
451 was not provided for the Colombian dataset so plots were selected based on the forest type, and
452 these plots were excluded from analyses requiring elevation. To avoid double counting plots,
453 Venezuelan and Colombian plots were removed from the ref.² dataset.

454

455 **Aboveground carbon**

456 For each tree in the montane dataset we used the published allometric equation by ref.⁵⁴ to
457 estimate aboveground biomass. This allometric equation was created using data from directly
458 harvested trees at 58 sites across the tropics, including eight sites with elevation ≥800m asl (range
459 900-3,000m asl including sites in Africa). We then converted this biomass to carbon, assuming that

460 aboveground carbon (AGC, in Mg C ha^{-1}) is 45.6% of aboveground biomass⁵⁵. AGC for each plot was
461 estimated as the sum of the AGC of each living stem, divided by planimetric plot area (in hectares). If
462 field measurements of slope were unavailable, we converted surface to planimetric area extracting
463 slope from the NASA's Shuttle Radar Topography Mission (SRTM) product. We excluded tree ferns,
464 bamboo and palms, as these were not measured in all plots. Ref.⁵⁴ includes tree diameter, wood
465 mass density and tree height. The best taxonomic match wood density of each stem was extracted
466 from a global database^{56,57} following ref.⁵³. For some sites, all trees in a plot had been sampled for
467 height. If this was not the case, but some field measurements of height were available (typically ten
468 stems per diameter class), we constructed a site-specific height-diameter model, using a Weibull
469 equation following ref.⁵⁸. If no field measurements of height were available, we constructed a
470 cluster-specific height-diameter model, using a Weibull equation, as explained in Table S7 in
471 Supplementary Information. The same approach was used to calculate aboveground biomass for
472 lowland forests. For these, height was estimated using a Weibull equation following ref.⁵⁸.

473

474 **Small plots and data subsampling**

475 For 22 sites where plots were small (<0.2 ha), we aggregated plots to groups of about 0.2 ha based
476 on their geographic proximity, elevation, environmental affinity and the co-authors' knowledge of
477 the site, to help reduce the variation among plots at site level. This is because the presence of an
478 extremely large tree in a small plot can result in overestimates of AGC⁵⁹. We investigated if using the
479 aggregated-plot approach affected AGC-stock estimates at the site level, and this was not the case
480 (Extended Data Fig. 2). We also investigated if including small plots affected the continental mean
481 AGC-stock estimates, as small plots have greater edge surface, and there is a tendency of some field
482 teams to include large trees inside plots when laying out the boundaries⁶⁰. Including small plots did
483 not significantly affect our continental mean AGC-stock estimates (Extended Data Fig. 2). We also
484 explored the sensitivity of our continental mean AGC-stock estimates to data subsampling. Data
485 were resampled at different sample sizes either at plot level (sampling with replacement) or at site
486 level (sampling without replacement). The number of plots ($n=226$) and the number of sites ($n=44$)
487 we sampled indicate that our estimates of AGC-stock at the continental level are robust (Extended
488 Data Fig. 1). They are also not affected by the fact that we included plots 800-1,000 m asl (Extended
489 Data Fig. 3).

490

491 **Size classes**

492 For all plots, we computed the proportion of AGC which was distributed in each size-diameter class,
493 using the classes of ref.¹⁵. We also computed stem density, basal area, density of large trees (>70 cm
494 diameter, named SD_{70} in stems ha^{-1}) and Podocarpaceae abundance (in percentage of plot-level
495 basal area).

496

497 **Environmental variables and their effects**

498 Climate variables (temperature annual mean and seasonality, and precipitation mean and
499 seasonality, i.e. Bio1, 4, 12 and 15) were extracted from WorldClimV2⁶¹ at 30 arc-sec (~ 1 -km)
500 resolution. Mean temperature values were adjusted for the difference in elevation between the plot
501 and the wider 1-km grid cell using the lapse rate of $-0.005^\circ\text{C m}^{-1}$. We obtained data on cloud cover
502 from ref.⁶² and lightning frequency (0.1 degree, ~ 11 km) from the Lightning Imaging Sensor (LIS) very
503 high resolution climatology⁶³. Values for soil variables (cation exchange capacity, CEC, representing
504 soil fertility, and percentage clay representing soil texture) were extracted from SoilGrids⁶⁴ (~ 1 -km
505 resolution) and a depth-weighted mean taken for values from 0 to 30 cm depth to give a single value
506 of each soil variable per plot. Elevation was obtained from SRTM (at 3 arc-second resolution, ~ 90 m).
507 Topographic metrics were calculated from elevation data using the terrain function in the raster R
508 package version 3.3-6. These were slope and topographic position index (TPI). TPI is the difference
509 between the elevation of the plot and the mean value of the eight surrounding grid cells – positive
510 values indicate locally high locations and negative values indicate locally low locations. Where small

511 plots were aggregated for analysis, environmental variables were extracted for the ungrouped plot
512 locations, and then an area-weighted mean taken to obtain a plot-level value.

513

514 **Elephant and conifer effects on AGC-stocks**

515 For the current elephant presence in the AfriMont plots, we created a binary variable
516 (presence/absence) based on co-authors knowledge of elephant ranges and elevation distribution at
517 each site as of 2019. Co-authors estimated that elephants were present in 2019 in 54 plots in 12
518 sites in five countries (see Table S5). For all plots which had at least one individual in the
519 Podocarpaceae family (47 plots, 16 sites, 7 countries), we computed the contribution of
520 Podocarpaceae to plot basal area and AGC-stock in terms of percentages.

521

522 **Estimating forest cover and loss**

523 We obtained estimates of forest cover and loss in the years 2000 through to 2018, using the 'loss
524 year' dataset of the Global Forest Change database, version 1.6 (ref.³⁸). To exclude plantation
525 forests, 'dry' forests (e.g. miombo woodland) and degraded forests, we applied the 'primary humid
526 forest' mask developed by ref.³⁹. We distinguished montane from lowland forests using an
527 elevational cut-off of 800-m elevation, using the SRTM v3 product at 1 arc-sec resolution (snapping
528 to the ref.³⁸ grid of the same resolution). Where there were gaps in the 1 arc-sec SRTM product, we
529 filled these using a 1 arc-sec bilinear interpolation of the (gapless) 3 arc-sec SRTM product. Areal
530 estimates of forest cover and loss were calculated at 30-m resolution using the Africa Sinusoidal
531 projection. To estimate future forest loss by year 2030, we extrapolated absolute country-level
532 deforestation rates for the period 2000-2018 (in ha per year).

533

534 **Investigating AfriMont representativeness**

535 To quantify AfriMont sampling effort within the montane forest biome in Africa, we used the map of
536 tropical montane forest extent (see above) and calculated the amount of remaining forest in each 1-
537 degree grid-cell. By dividing the area sampled in the AfriMont dataset by the proportion of this
538 biome in a grid-cell, we calculated the expected sampling intensity if sampling was proportional to
539 remaining forest extent. To assess how representative our plot network was of the environmental
540 conditions of the wider tropical montane forest biome in Africa, we extracted the environmental
541 data (climate and soil variables presented above) at ~1-km resolution from grid-cells that contained
542 montane forest. We then visually compared the distribution of each variable in our dataset to its
543 distribution across the biome (Extended Data Fig. 7).

544

545 **AfriMont vs global AGC maps**

546 We extracted alternative AGC estimates for the AfriMont plots (unaggregated, n=666) from four
547 different sources: Harris et al. (ref.⁶⁵) (30-m resolution, dated 2000), the European Space Agency
548 Climate Change Initiative Biomass map⁶⁶ (100-m resolution, 2017), Saatchi, et al. (ref.⁶⁷) (1-km
549 resolution, 2007/8) and Avitabile et al. (ref.⁶⁸) (1-km resolution, circa 2000-2010). Most of the
550 AfriMont plots were sampled between 2000 and 2019 (Table S5). Where the plots were found within
551 a single map pixel, we extracted that value. Where plots were larger than the pixel size, we averaged
552 the values from the surrounding pixels weighted according to the proportion of the pixel that was in
553 the plot.

554

555 **Statistical analysis**

556 Data were analysed using linear mixed-effects models, with site as a random effect. Site was
557 included as a random intercept in all models, and as a random slope where relationships were
558 assessed against elevation. Allowing the slope of the elevation effect to vary amongst sites in this
559 way captures the *a priori* expectation for slopes to differ among sites, for example due to mass
560 elevation effects. The effect of plot size on variation was accounted for by weighting observations by
561 a power transformation of plot size; this was estimated during model fitting using the varPower

562 function in the nlme R package (ref.⁶⁹), and then models refitted using the lme4 R package (ref.⁷⁰)
563 using these estimated weights. Confidence intervals and *P*-values for mixed effects models
564 parameters were estimated by bootstrapping models (1,000 iterations) using the
565 bootstrap_parameters function in the parameters R package (ref.⁷¹). AGC-stocks, stem density and
566 SD₇₀ were natural-log transformed (a small constant was added to SD₇₀ before log transforming to
567 avoid log-transforming zeros) to meet assumptions of normality and avoid heteroscedacity. Likewise,
568 the proportional contribution of each size class was square-root transformed. Differences in AGC-
569 stocks between all combinations of lowland and montane forests amongst continents were assessed
570 using Tukey post-hoc tests implemented in the multcomp R package (ref.⁷²). Relationships between
571 AGC-stocks and environmental variables were investigated by fitting all subsets of the full model
572 with all environmental covariates and averaging the best supported (difference in Akaike
573 information criterion from the best supported model $\Delta AIC < 4$) models (using dredge and model.avg
574 functions in the MuMIn R package (ref.⁷³). We used these relationships with climate and soil to
575 predict AGC-stocks in each 1-km grid cell containing montane forests (holding topographic variables
576 at their dataset wide mean), and then took the forest-area weighted mean of these to obtain a
577 single mean for the tropical montane forest biome in Africa. Differences in AGC-stocks between
578 plots with and without elephants were tested using t-test with AGC-stocks natural-log transformed.
579 We investigated if Podocarpaceae abundance (in terms of basal area) and plot AGC-stocks were
580 significantly correlated using Spearman's rank correlation coefficient. To investigate if sampling
581 design affected AfriMont AGC-stock estimates we used ANOVA to test whether site-level mean AGC-
582 stocks differed according to the sampling strategy used to establish plots at that site. To explore the
583 relationship between AfriMont AGC-stock estimates and global maps, and among these global maps,
584 we used Spearman's rank correlation test.

585

586 **References Methods**

- 587 50. Lopez-Gonzalez, G., Lewis, S. L., Burkitt, M. & Phillips, O. L. ForestPlots.net: a web application
588 and research tool to manage and analyse tropical forest plot data. *J. Veg. Sci.* **22**, 610–613
589 (2011).
- 590 51. Lopez-Gonzalez, G., Lewis, S. L., Burkitt, M., Baker, T. R. & Phillips, O. L. ForestPlots.net
591 Database <http://www.forestplots.net> (2009).
- 592 52. Cavanaugh, K., et al. Carbon storage in tropical forests correlates with taxonomic diversity
593 and functional dominance on a global scale. *Global Ecol. Biogeogr.* **23**, 563–573 (2014).
- 594 53. Lewis, S. L., et al. 2009 Increasing carbon storage in intact African tropical forests. *Nature*
595 **457**, 1003–1006 (2009).
- 596 54. Chave, J. et al. Improved allometric models to estimate the aboveground biomass of tropical
597 trees. *Glob. Change Biol.* **20**, 3177–3190 (2014).
- 598 55. Martin, A. R., Doraisami, M. & Thomas, S. C. Global patterns in wood carbon concentration
599 across the world's trees and forests. *Nat. Geosci.* **11**, 915–920 (2018).
- 600 56. Chave, J. et al. Towards a worldwide wood economics spectrum. *Ecol. Lett.* **12**, 351–366
601 (2009).
- 602 57. Zanne, A. E. et al. Towards a Worldwide Wood Economics Spectrum
603 <https://doi.org/10.5061/dryad.234> (Dryad Digital Repository, 2009).
- 604 58. Clark, D.A., Brown, S., Kicklighter, D.W., Chambers, J.Q., Thomlinson, J.R., Ni, J. & Holland,
605 E.A. Net primary production in tropical forests: an evaluation and synthesis of existing field
606 data. *Ecol. Appl.* **11**, 371–384 (2001).
- 607 59. Paul, T.S.H., Kimberley, M.O. & Beets, P.N. Thinking outside the square: Evidence that plot
608 shape and layout in forest inventories can bias estimates of stand metrics. *Methods Ecol.*
609 *Evol.* **10**, 381–388 (2019).
- 610 60. Fick, S.E. & Hijmans, R.J., WorldClim 2: new 1-km spatial resolution climate surfaces for
611 global land areas. *Int. J. Climatol.* **37**, 4302–4315 (2017).

- 612 61. Wilson, A.M. & Jetz, W. Remotely sensed high-resolution Global Cloud Dynamics for
613 predicting ecosystem and biodiversity distributions. *PLoS Biol* **14**(3): e1002415 (2016).
- 614 62. Albrecht, R., Goodman, S., Buechler, D., Blakeslee R. & Christian, H. LIS 0.1 Degree Very High
615 Resolution Gridded Lightning Climatology Data Collection. Data sets available online
616 [<https://ghrc.nsstc.nasa.gov/pub/lis/climatology/LIS/>] from the NASA Global Hydrology
617 Resource Center DAAC, Huntsville, Alabama, U.S.A. doi:
618 <http://dx.doi.org/10.5067/LIS/LIS/DATA306>
- 619 63. Hengl, T., et al. SoilGrids250m: Global gridded soil information based on machine learning.
620 *PLoS ONE* **12**(2): e0169748 (2017).
- 621 64. Harris, N. L. et al. Global maps of twenty-first century forest carbon fluxes. *Nat. Clim. Change*
622 **11**, 234–240 (2021).
- 623 65. Santoro, M. & Cartus, O. ESA Biomass Climate Change Initiative (Biomass_cci): Global
624 datasets of forest above-ground biomass for the year 2017, v1. Centre for Environmental
625 Data Analysis, 2019. doi:10.5285/bedc59f37c9545c981a839eb552e4084
- 626 66. Saatchi, S., et al. Benchmark map of forest carbon stocks in tropical regions across three
627 continents. *PNAS* **108**, 9899–9904 (2011).
- 628 67. Avitabile, V., et al. An integrated pan-tropical biomass map using multiple reference
629 datasets. *Glob. Change Biol.* **22**, 1406–1420 (2016).
- 630 68. Pinheiro, J., Bates, D., DebRoy, S., Sarkar, D. & R Core Team. nlme: Linear and Nonlinear
631 Mixed Effects Models. R package version 3.1-151, <https://CRAN> (2020).
- 632 69. Bates, D. Maechler, M., Bolker B. & Walker, S. Fitting Linear Mixed-Effects Models Using
633 lme4. *J. Stat. Softw.* **67**, 1–48 (2015).
- 634 70. Lüdtke, D., Ben-Shachar, M., Patil, I. & Makowski, D. Parameters: extracting, computing
635 and exploring the parameters of statistical models using R. *J. Open Source Softw* **5**, 2445
636 (2020).
- 637 71. Hothorn, T., Bretz, F. & Westfall, P. Simultaneous Inference in General Parametric Models.
638 *Biometrical Journal* **50**, 346–363 (2008).
- 639 72. Barton, K. 2020. MuMIn: Multi-Model Inference. R package version 1.43.17.

640

641 **Acknowledgements**

642 We sincerely thank the people of the many villages and local communities who welcomed our field
643 teams and became our field assistants, without whose support the AfriMont dataset would not have
644 been possible. *Cameroon*: villages Elak-Oku, Bokwoango, Bakingili, Muandelengoh, Enyandong,
645 Ekangmbeng, Ngalmoa, Dikome Balue, Muyange, Matamani; assistants: E. Ndivi, D. Wultof, F.
646 Keming, E. Bafon, J. Meyeih, T. K. Konsum, J. Esembe, F. Luma, F. Teke, E.E. Dagobert, E.D. Ndode,
647 N.F. Njikang; *DRC*: Bunyakiri, J. Kalume, W. Gului, D. Cirhagaga, B. Mugisho; *Kenya*: assistants: A.M.
648 Aide, H. Lerapo, J. Harugura, R.A. Wamuro, J. Lekatap, L. Lemooli, D. Kimuzi, B.M. Lombo, J. Broas, J.
649 Hietanen, V. Heikinheimo, E. Schäfer; *Rwanda*: assistants: I. Rusizana, P. Niyontegereje, J.B. Gakima,
650 F. Ngayabahiga; *Tanzania*: TEAM staff and affiliates; *Uganda*: K. Laughlin, X. Mugumya, L. Etwodu, M.
651 Mugisa.

652

653 For logistical and administrative support, we are indebted to international, national and local
654 institutions: SOPISDEW, Mt Cameroon National Park, Tropical Plant Exploration Group (TroPEG),
655 Institut Congolais de Conservation de la Nature, Kahuzi-Biega National Park, Itombwe Nature
656 Reserve, NEMA Marsabit Office, Taita Research Station, Kenya Forest Service, Rwanda Development
657 Board, Nyungwe National Park, Conservation International, the Smithsonian Institution, Wildlife
658 Conservation Society, Sokoine University of Agriculture, Tanzania Wildlife Research
659 Institute, Tanzania National Parks Authority, Kilimanjaro National Park, Tanzania Commission for
660 Science and Technology, Royal Zoological Society of Scotland, Uganda Wildlife Authority, Makerere
661 University Biological Field Station, Uganda National Forestry Authority, Uganda National Council for
662 Science and Technology.

663

664 Field campaigns for AfriMont were funded by Marie Skłodowska-Curie Actions Intra-European
665 Fellowships (number 328075) and Global Fellowships (number 74356), National Geographic Explorer
666 (NGS-53344R-18), Czech Science Foundation (no. 21-17125S), Rufford Small Grant Foundation
667 (16712-B, 19476-D), Ministry of Foreign Affairs of Finland (BIODEV project), the Academy of Finland
668 (number 318645), Swedish International Development Cooperation Agency, the Leverhulme Trust,
669 the Strategic Research Area Biodiversity and Ecosystem Services in a Changing Climate, the German
670 Research Foundation (DFG), Gatsby Plants, Natural Science and Engineering Research Council of
671 Canada and International Development Research Centre of Canada.

672

673 This paper is also a product of the AfriTRON network, for which we are indebted to hundreds of
674 institutions, field assistants and local communities for establishing and maintaining the plots,
675 including: the Forestry Development Authority of the Government of Liberia, the University of
676 Liberia, University of Ibadan (Nigeria), the University of Abeokuta (Nigeria), the University of
677 Yaounde I (Cameroon), the National Herbarium of Yaounde (Cameroon), the University of Buea
678 (Cameroon), Bioversity International (Cameroon), Salonga National Park (Democratic Republic of
679 Congo), The Centre de Formation et de Recherche en Conservation Forestière (CEFRECOF, Epulu,
680 Democratic Republic of Congo), the Institut National pour l'Étude et la Recherche Agronomiques
681 (INERA, Democratic Republic of Congo), the École Régionale Postuniversitaire d'Aménagement et de
682 Gestion intégrés des Forêts et Territoires tropicaux (ERAIFT Kinshasa, Democratic Republic of
683 Congo), WWF-Democratic Republic of Congo, WCS-Democratic Republic of Congo, the Université de
684 Kisangani (Democratic Republic of Congo), Université Officielle de Bukavu (Democratic Republic of
685 Congo), Université de Mbuji-Mayi (Democratic Republic of Congo), le Ministère de l'Environnement et
686 Développement Durable (Democratic Republic of Congo), the FORETS project in Yangambi (CIFOR,
687 CGIAR and the European Union; Democratic Republic of Congo), the Lukuru Wildlife Research
688 Foundation (Democratic Republic of Congo), Mbarara University of Science and Technology (MUST,
689 Uganda), WCS-Uganda, the Uganda Forest Department, the Commission of Central African Forests
690 (COMIFAC), the Udzungwa Ecological Monitoring Centre (Tanzania) and the Sokoine University of
691 Agriculture (Tanzania). The AfriTRON network has been supported by the European Research
692 Council (291585, 'T-FORCES' – Tropical Forests in the Changing Earth System, Advanced Grant to
693 O.L.P. and S.L.L.), the Gordon and Betty Moore Foundation, the David and Lucile Packard
694 Foundation, the European Union's Seventh Framework Programme (283080, 'GEOCARBON').

695

696 We are particularly grateful to A. Daniels, F. Mbayu, T.R. Feldpausch, E. Kearsley, J. Lloyd, R. Lowe, J.
697 Mukinzi, L. Ojo, A.T. Peterson, J. Talbot and L. Zemagho for giving us access to their plot data. We
698 also thank C. Chatelain (Geneva Botanic Gardens) for access to the African Plants Database and to H.
699 Tang for helping explore the use of GEDI data.

700

701 Data from AfriTRON and most of AfriMont are stored and curated by ForestPlots.net, a long-term
702 cyberinfrastructure initiative hosted at the University of Leeds that unites permanent plot records
703 and their contributing scientists from the world's tropical forests. The development of
704 ForestPlots.net and curation of African data have been funded by many sources, including the ERC
705 (principally from AdG 291585 'T-FORCES'), the UK Natural Environment Research Council (including
706 NE/B503384/1, NE/F005806/1, NE/P008755/1, NE/N012542/1 and NE/I028122/1), the Gordon and
707 Betty Moore Foundation ('RAINFOR', 'MonANPeru'), the EU Horizon programme (especially
708 'GEOCARBON', 'Amazalert') and the Royal Society (University Research Fellowship to S.L.L.).

709

710 **Author Contributions**

711 A.C-S. conceived the study and assembled the AfriMont dataset. A.C-S. and M.J.P.S. analysed the
712 plot data (with contributions from S.L.L.) and wrote the manuscript. P.J.P. analysed forest extents
713 and contributed to writing. S.L.L. conceived and managed the AfriTRON forest plot census

714 programme. E.T.A.M. and V.A. helped compare plot data with remote sensing carbon maps. All co-
715 authors read and approved the manuscript.

716

717 **Competing interests** The authors declare no competing interests.

718

719 **Additional information**

720 Supplementary information is available for this paper at XX (to be added)

721 Correspondence and requests for materials should be addressed to A. C-S.

722 Reprints and permissions information are available at XX (to be added)

723

724 **Data availability**

725 Source data to generate figures and tables are available from:

726 https://doi.org/10.5521/forestplots.net/2021_5

727

728 **Code availability**

729 R code to generate figures and tables is available from:

730 https://doi.org/10.5521/forestplots.net/2021_5

731

732 **Affiliations**

733 ¹Department of Environment and Geography, University of York, York, UK. ²Department of
734 International Environmental and Development Studies (NORAGRIC), Norwegian University of Life
735 Sciences, Ås, Norway. ³Department of Natural Sciences, Manchester Metropolitan University,
736 Manchester, UK. ⁴School of Geography, University of Leeds, Leeds, UK. ⁵Climate Change Specialist
737 Group, Species Survival Commission, International Union for Conservation of Nature, Gland,
738 Switzerland. ⁶University College London, Department of Geography, London, UK. ⁷Biology
739 Department, Université Officielle de Bukavu, Bukavu, DRC. ⁸Service of Wood Biology, Royal Museum
740 for Central Africa, Tervuren, Belgium. ⁹Department of Environment, Laboratory of Wood Technology
741 (Woodlab), Ghent University, Ghent, Belgium. ¹⁰University of Jos, Jos, Nigeria. ¹¹Nigerian Montane
742 Forest Project, Taraba State, Nigeria. ¹²Department of Geosciences and Geography, University of
743 Helsinki, Finland. ¹³Department of Zoology, Faculty of Science, Charles University, Prague, Czech
744 Republic. ¹⁴Institute of Vertebrate Biology, Czech Academy of Sciences, Brno, Czech Republic.
745 ¹⁵Institute of Botany of the Czech Academy of Science, Třeboň, Czech Republic. ¹⁶College of Natural
746 and Computational Science, Addis Ababa University, Addis Ababa, Ethiopia. ¹⁷Department of Natural
747 Resource Management, College of Agriculture and Natural Resource, Wolkite University, Wolkite,
748 Ethiopia. ¹⁸European Commission, Joint Research Centre, Ispra, Italy. ¹⁹UK Centre for Ecology &
749 Hydrology, Edinburgh, UK. ²⁰Université du Cinquantenaire Lwiro, Département de sciences de
750 l'environnement, Kabare, Suk-Kivu, DRC. ²¹Isotope Bioscience Laboratory (ISOFYS), Ghent University,
751 Ghent, Belgium. ²²Plant Systematic and Ecology Laboratory, Higher Teachers' Training College,
752 University of Yaoundé I, Yaoundé, Cameroon. ²³Institute of Tropical Forest Conservation, Mbarara
753 University of Science and Technology, Uganda. ²⁴Biodiversity and Landscape Unit, Gembloux Agro-
754 Bio Tech, Université de Liège, Liège, Belgium. ²⁵Institut für Geographie, Friedrich-Alexander-
755 Universität, Erlangen-Nürnberg, Germany. ²⁶Institut Supérieur d'Agroforesterie et de Gestion de
756 l'Environnement de Kahuzi-Biega (ISAGE-KB); Département de Eaux et Forêts, Kalehe, DRC. ²⁷UN
757 Environment World Conservation Monitoring Center (UNEP-WCMC), Cambridge, UK.
758 ²⁸Computational & Applied Vegetation Ecology (CAVELab), Faculty of Bioscience Engineering, Ghent
759 University, Ghent, Belgium. ²⁹Department of Anthropology, George Washington University,
760 Washington DC, USA. ³⁰School of Life Sciences, University of KwaZulu-Natal, Scottsville,
761 Pietermaritzburg, South Africa. ³¹Shaaxi Key Laboratory for Animal Conservation, Northwest
762 University, Xi'an, China. ³²International Centre of Biodiversity and Primate Conservation, Dali
763 University, Dali Yunnan, China. ³³University of Canterbury, New Zealand. ³⁴Inventory & Monitoring
764 Program, National Park Service, Fredericksburg, USA. ³⁵University of Ghent, Belgium. ³⁶World

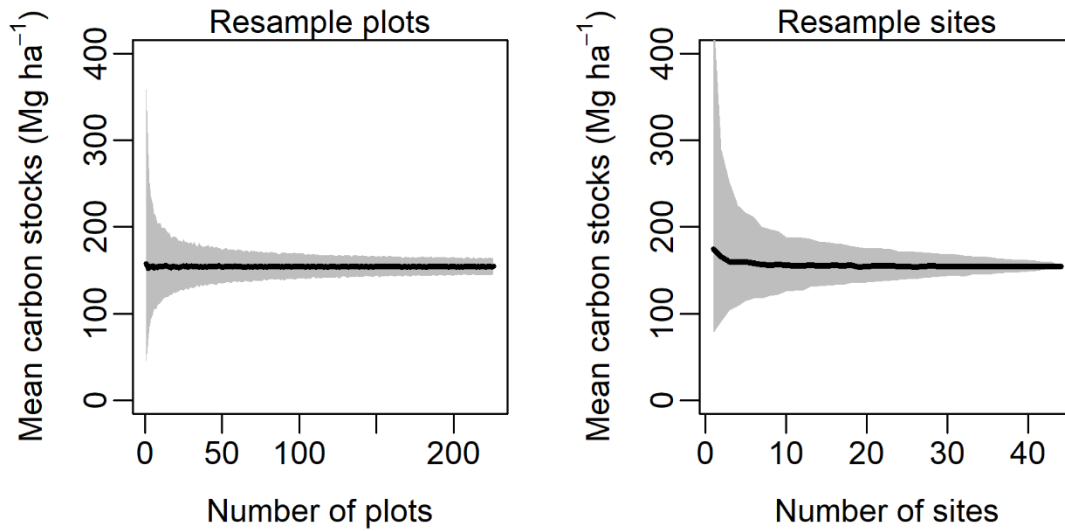
765 Agroforestry (ICRAF), Nairobi, Kenya. ³⁷Laboratory of Geo-Information Science and Remote Sensing,
766 Wageningen University, Wageningen, the Netherlands. ³⁸Geography, Environment & Geomatics,
767 University of Guelph, Canada. ³⁹Faculty of Science, University of South Bohemia, České Budějovice,
768 Czech Republic. ⁴⁰AMAP Lab, Université de Montpellier, IRD, CNRS, INRAE, CIRAD, Montpellier,
769 France. ⁴¹Faculté de Gestion de Ressources Naturelles Renouvelables, Université de Kisangani,
770 Kisangani, DRC. ⁴²College of Development Studies, Addis Ababa University, Ethiopia.
771 ⁴³Dendrochronology Laboratory, World Agroforestry Centre (ICRAF), Kenya. ⁴⁴Missouri Botanical
772 Garden, St. Louis, Missouri, USA. ⁴⁵Department of Biology, University of Burundi, Burundi.
773 ⁴⁶Smithsonian Institution Forest Global Earth Observatory (ForestGEO), Smithsonian Tropical
774 Research Institute, Washington DC, USA. ⁴⁷Kunming Institute of Botany, Kunming, China. ⁴⁸Université
775 Libre de Bruxelles, Brussels, Belgium. ⁴⁹Division of Vertebrate Zoology, Yale Peabody Museum of
776 Natural History, New Haven, CT, USA. ⁵⁰Institute for Atmospheric and Earth System Research, Faculty
777 of Science, University of Helsinki, Finland. ⁵¹Department of Plant Systematics, University of Bayreuth,
778 Germany. ⁵²Institute for Geography, Friedrich-Alexander-University Erlangen-Nuremberg, Germany.
779 ⁵³Helmholtz-Centre for Environmental Research (UFZ), Leipzig, Germany. ⁵⁴Department of Ecology,
780 Faculty of Science, Charles University, Prague, Czech Republic. ⁵⁵International Gorilla Conservation
781 Programme, Musanze, Rwanda. ⁵⁶Department of Natural Resources, Karatina University, Kenya.
782 ⁵⁷Dept. Ecosystem Science & Sustainability, Colorado State University, Fort Collins, USA.
783 ⁵⁸Eco2librium LLC, Boise, USA. ⁵⁹Department of Ecology, Université de Kisangani, Kisangani, DRC.
784 ⁶⁰Environmental Change Institute, School of Geography and the Environment, University of Oxford,
785 Oxford, UK. ⁶¹Tropical Forests and People Research Centre, University of the Sunshine Coast,
786 Australia. ⁶²Flamingo Land Ltd., North Yorkshire, UK. ⁶³College of African Wildlife Management,
787 Mweka, Tanzania. ⁶⁴School of GeoSciences, University of Edinburgh, UK. ⁶⁵Department of Geography
788 and Environmental Sciences, University of Dundee, Dundee, UK. ⁶⁶Independent Botanist, Harare,
789 Zimbabwe. ⁶⁷Department of Horticultural Sciences, Faculty of Applied Sciences, Cape Peninsula
790 University of Technology, Bellville, South Africa. ⁶⁸Biology Department, University of Rwanda,
791 Rwanda. ⁶⁹Department of Biological and Environmental Sciences, University of Gothenburg, Sweden.
792 ⁷⁰Mountains of the Moon University, Fort Portal, Uganda. ⁷¹National Agricultural Research
793 Organisation, Mbarara Zonal Agricultural Research and Development Institute, Mbarara, Uganda.
794 ⁷²School of Biological Sciences, University of Southampton, Southampton, UK. ⁷³Conservation
795 Science Group, Department of Zoology, University of Cambridge, Cambridge, UK. ⁷⁴State Key
796 Laboratory of Information Engineering in Surveying, Mapping and Remote Sensing, Wuhan
797 University, China. ⁷⁵Key Biodiversity Areas Secretariat, BirdLife International, Cambridge, UK.
798 ⁷⁶School of Life Sciences, University of Lincoln, UK. ⁷⁷Department of Biology, University of Florence,
799 Sesto Fiorentino, Italy. ⁷⁸Tropical Biodiversity Section, Museo delle Scienze, Trento, Italy. ⁷⁹Tropical
800 Plant Exploration Group (TroPEG) Cameroon. ⁸⁰Center for Development Research (ZEF), University of
801 Bonn, Germany. ⁸¹Conservation and Landscape Ecology, University of Freiburg, Germany. ⁸²Applied
802 Biology and Ecology Research Unit, University of Dschang, Dschang, Cameroon. ⁸³Forest Ecology and
803 Forest Management Group, Wageningen University, Wageningen, The Netherlands. ⁸⁴Water and
804 Land Resources Center, Addis Ababa University, Addis Ababa, Ethiopia. ⁸⁵African Wildlife Foundation
805 (AWF), Biodiversity Conservation and Landscape Management Program, Simien Mountains National
806 Park, Debark, Ethiopia. ⁸⁶Faculty of Forestry, University of British Columbia, Vancouver, Canada.
807 ⁸⁷Center for International Forestry Research (CIFOR), Bogor, Indonesia. ⁸⁸Department of Forest
808 Ecology, Faculty of Forestry and Wood Sciences, Czech University of Life Sciences, Prague, Czech
809 Republic. ⁸⁹Department of Plant Biology, Faculty of Sciences, University of Yaoundé I, Cameroon.
810 ⁹⁰Bioversity International, Yaoundé, Cameroon. ⁹¹UK Research & Innovation, UK. ⁹²Department of
811 Geography, National University of Singapore, Singapore. ⁹³Institute of Forestry and Conservation,
812 University of Toronto, Toronto, Canada. ⁹⁴Biodiversity Foundation for Africa, East Dean, East Sussex,
813 UK. ⁹⁵Forestry Development Authority of the Government of Liberia (FDA), Monrovia, Liberia.
814 ⁹⁶School of Forestry and Environmental Studies, Yale University, New Haven, USA. ⁹⁷Department of
815 Biological Sciences, Florida International University, Florida, USA. ⁹⁸School of Natural Sciences,

816 University of Bangor, Bangor, UK. ⁹⁹Rothamsted Research, Harpenden, UK. ¹⁰⁰University of Liberia,
817 Monrovia, Liberia. *corresponding author: a.cuni-sanchez@york.ac.uk

818

819 **Extended Data**

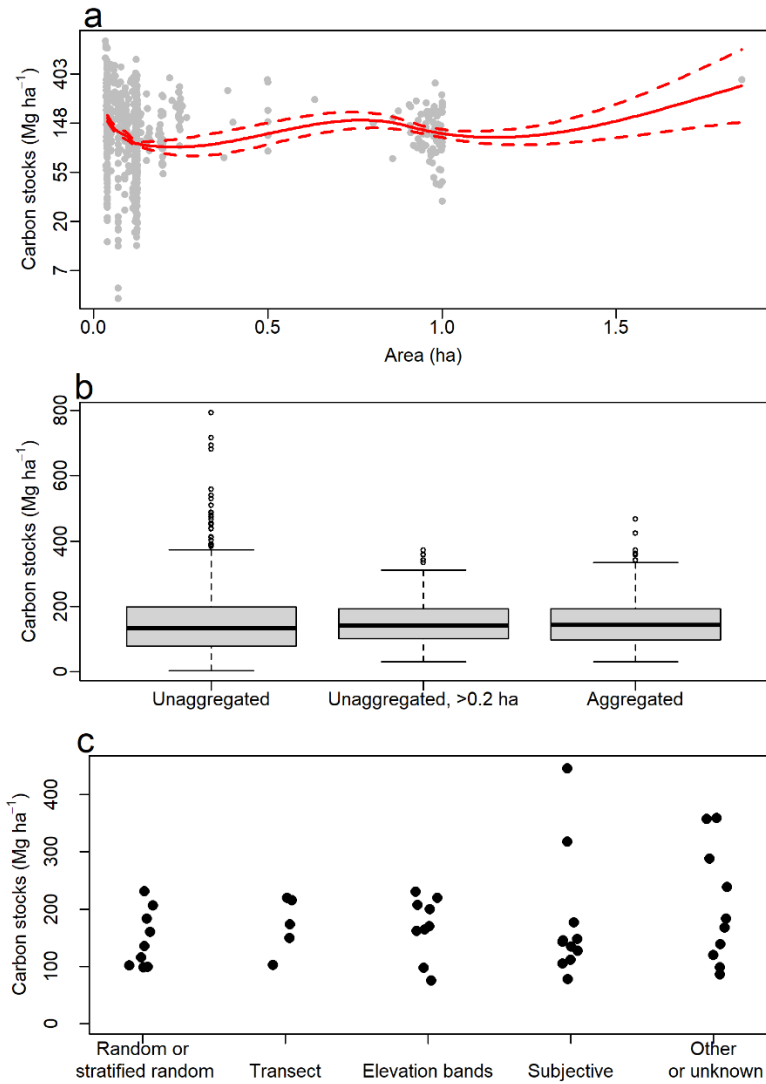
820



821

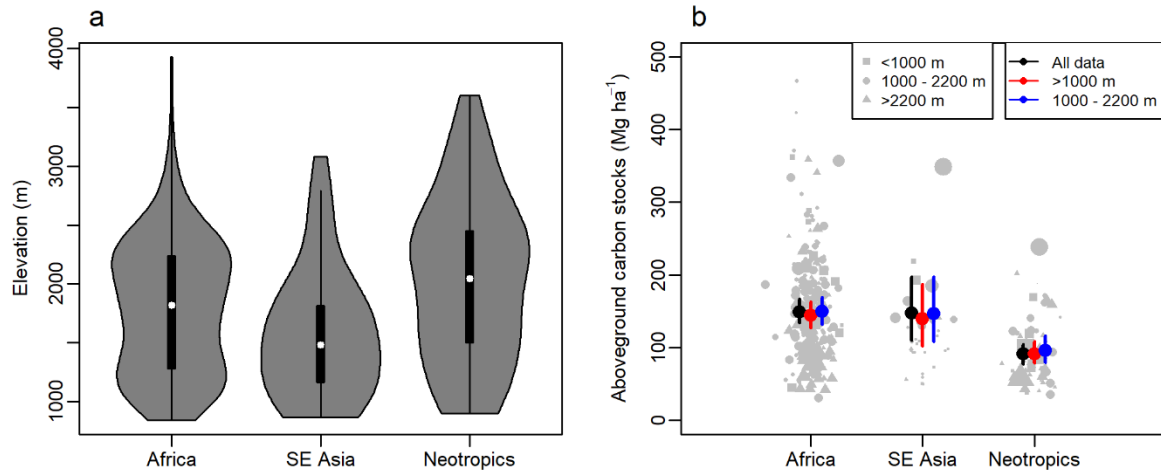
822 **Extended Data Fig. 1 | Sensitivity of mean aboveground carbon stock estimates to data**
823 **subsampling.** AfriMont plot data were resampled at different sample sizes either at plot level
824 (sampling with replacement) or at site level (sampling without replacement). $N = 1,000$ resamples
825 for each sample size.

826

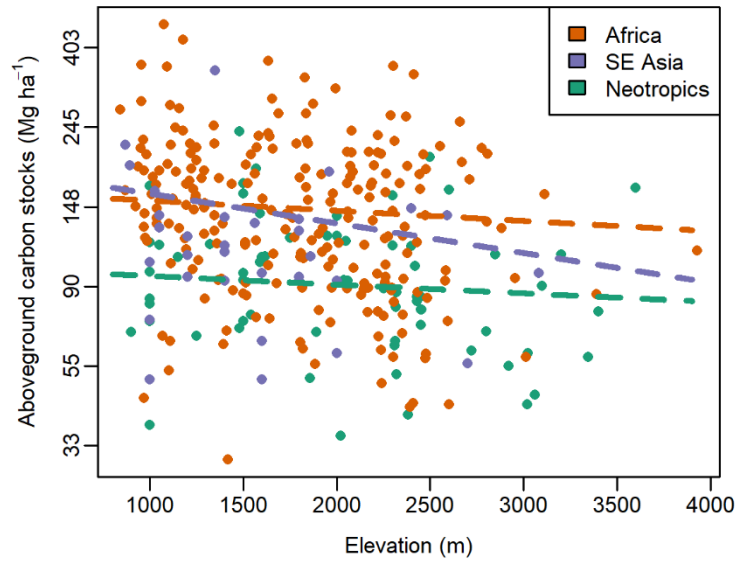


827
 828 **Extended Data Fig. 2 | Effect of plot area, aggregation procedure and plot design on estimates of**
 829 **aboveground carbon stocks across the AfriMont plot network. (a)** Relationship between
 830 aboveground carbon stocks and plot area of plots prior to aggregation. The red line shows the fit of a
 831 locally weighted regression model (span = 0.75) relating these variables, with dashed lines showing
 832 the standard errors. **(b)** Variation in aboveground carbon stocks using either all plots prior to
 833 aggregation (unaggregated), plots prior to aggregation but excluding those < 0.2 ha (unaggregated, >
 834 0.2 ha) or the aggregated plots used in the main analyses (aggregated). **(c)** Effects of plot design on
 835 aboveground carbon stocks (each site represents one dot). Sampling strategies include random or
 836 stratified random, plots positioned along transects, plots established within elevation bands,
 837 subjective measures such as choosing an area of forest considered representative of the wider area,
 838 and other strategies (one plot sampled per site or unclear strategy). Carbon stocks (log-transformed)
 839 did not differ significantly between sites with different sampling strategies (ANOVA: $F_{4,39} = 0.432$, P
 840 = 0.785). For specific site information see Table S5.

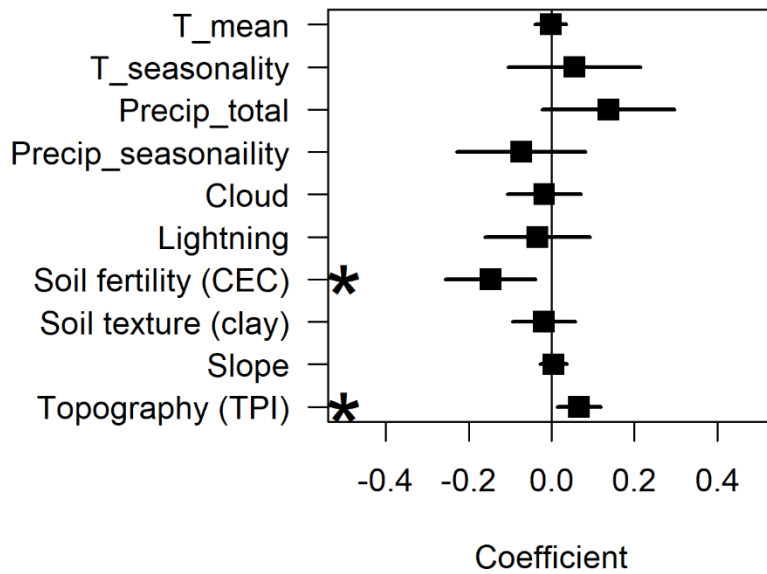
841
 842



843
 844 **Extended Data Fig. 3 | Robustness of differences in tropical montane forest aboveground carbon**
 845 **(AGC) stocks among continents based on plot networks to differences in elevation. (a)** Elevations
 846 of montane forests plots sampled in each continent. Violin plots show the distribution of data, with
 847 boxplots showing the median and interquartile range of elevation in each continent. **(b)** Effect of
 848 removing submontane plots (800-1,000 m asl) and high elevation plots (> 2,200 m asl, approximately
 849 the upper quartile of elevations for the African montane plot dataset) on AGC-stocks in montane
 850 forests sampled by plot networks in each continent. Mean AGC-stocks and 95% confidence intervals
 851 are shown as estimated by models using i) all data, ii) excluding plots 800-1,000 m, and iii) restricting
 852 plots to 1,000-2,200 m. Means for all plots differ from the analysis in Fig. 1 as literature plots without
 853 elevation data (plots in Colombia) were excluded from this analysis. Point symbols are proportional
 854 to square-root plot area. $N = 324$ plots.
 855
 856

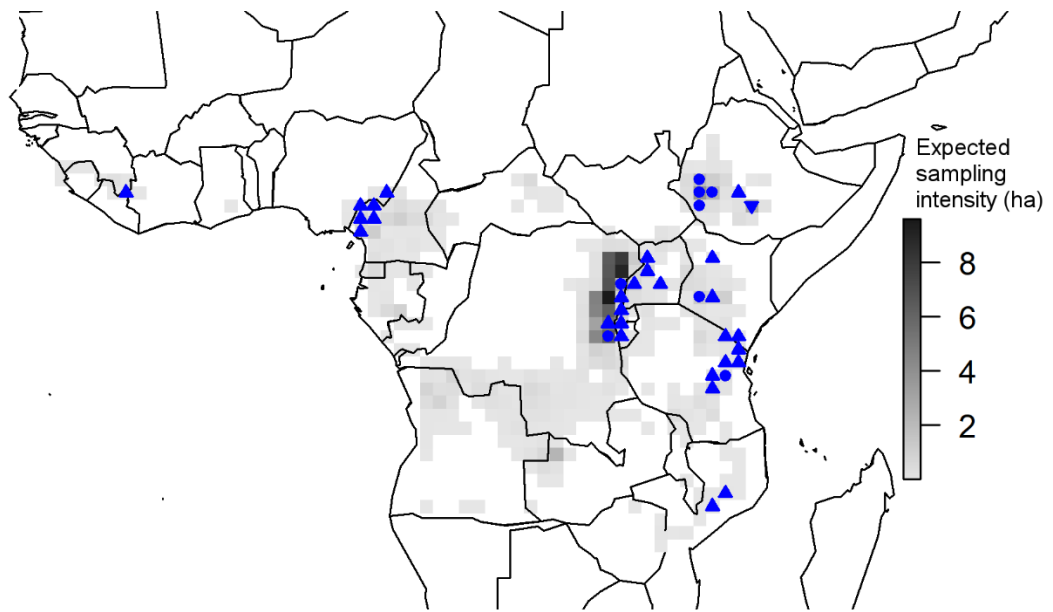


857
 858 **Extended Data Fig. 4 | Relationship between aboveground carbon (AGC) stocks and elevation for**
 859 **tropical montane forests in each continent based on plot networks.** Dashed lines show
 860 relationships from a linear mixed-effects model of log-transformed AGC-stocks as a function of
 861 elevation, continent and their interaction. Site was included as a random effect, and AGC-stock –
 862 elevation relationships allowed to vary among sites. Lines show fitted slopes across sites. Neither the
 863 overall relationship between elevation and AGC-stocks (slope = -0.039 [95% CI = -0.127 – 0.057], $P =$
 864 0.420) nor interactions between elevation and continent (Southeast Asia, change in slope = -0.074 [-
 865 0.294 – 0.149], $P = 0.503$; Neotropics, change in slope = 0.006 [-0.132 – 0.149], $P = 0.913$) are
 866 statistically significant. $N = 324$ plots.
 867
 868



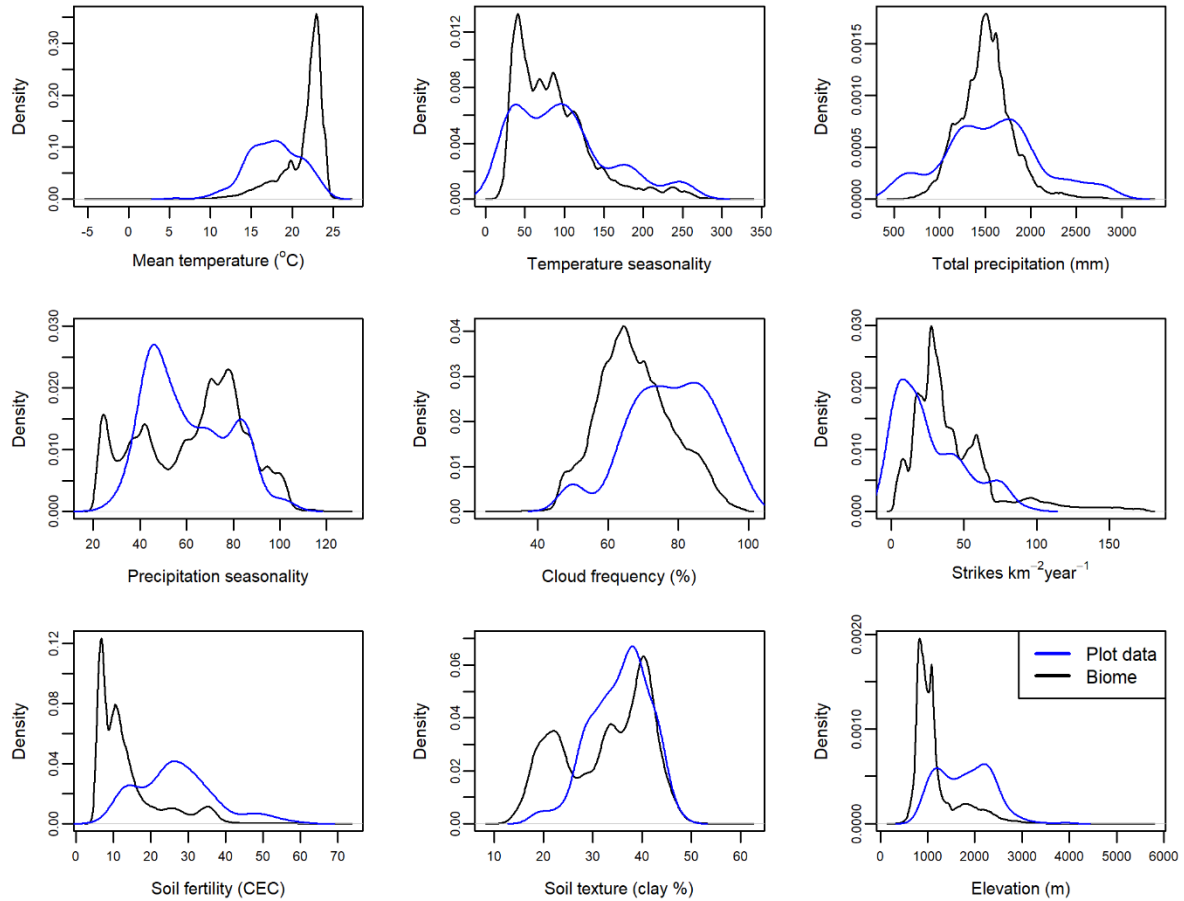
869
 870
 871
 872
 873
 874
 875
 876
 877
 878
 879

Extended Data Fig. 5 | Environmental drivers of aboveground carbon stocks across the AfriMont plot network. Coefficients are from a linear mixed-effects model with site as a random intercept. Results are following all-subsets regression and model averaging, in which variables that do not appear in well supported models are given coefficients of zero, leading to shrinkage in model coefficients. Statistically significant relationships ($P < 0.05$) are indicated with asterisks. TPI refers to topographic position index (positive values indicate higher than surroundings, negative values indicate lower than surroundings). T_mean: annual mean temperature, T_seasonality: temperature seasonality, Precip_total: annual precipitation, Precip_seasonality: precipitation seasonality.



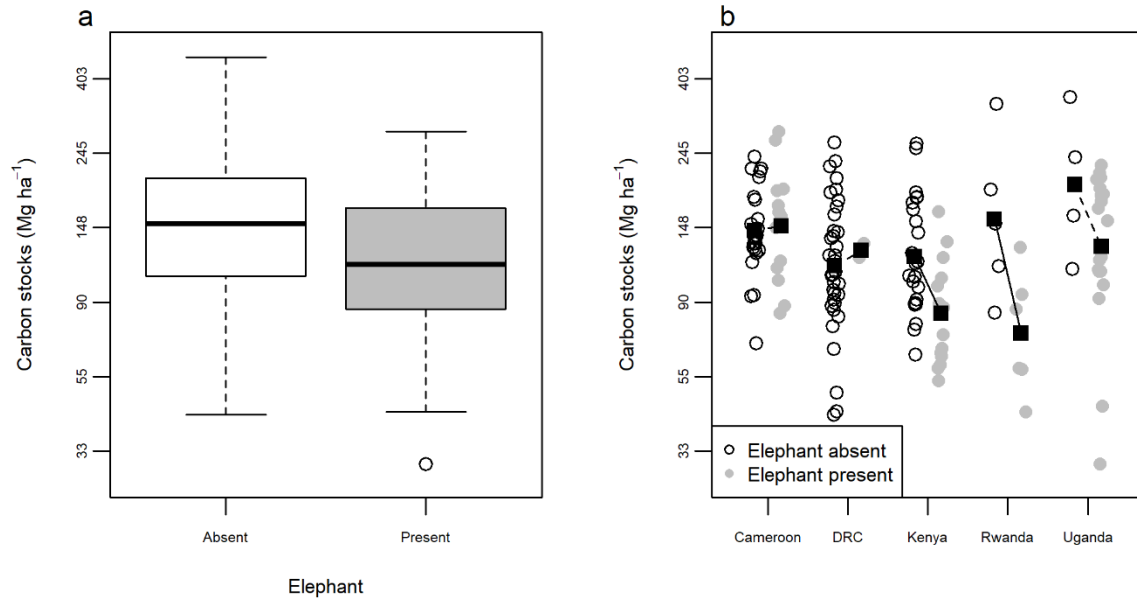
880
 881
 882
 883
 884
 885
 886
 887
 888
 889
 890

Extended Data Fig. 6 | Expected sampling effort if effort was distributed in proportion to the area of tropical montane forest biome in Africa. Data are summarised at 1-degree resolution. Upward triangles show grid-cells where AfriMont sampling effort is more than double expected effort, downward triangles show grid-cells where AfriMont sampling effort is less than half expected effort. Circles denote AfriMont sampling effort being between half and double expected effort. The extent of the tropical montane forest biome was defined as closed-canopy forests ≥ 800 m asl in December 2018, extracted from ref.³⁸ and clipped to 'primary humid forest' using ref.³⁹. This gridded map differs from Fig. 4 as numerous grids have very little tropical montane forest.



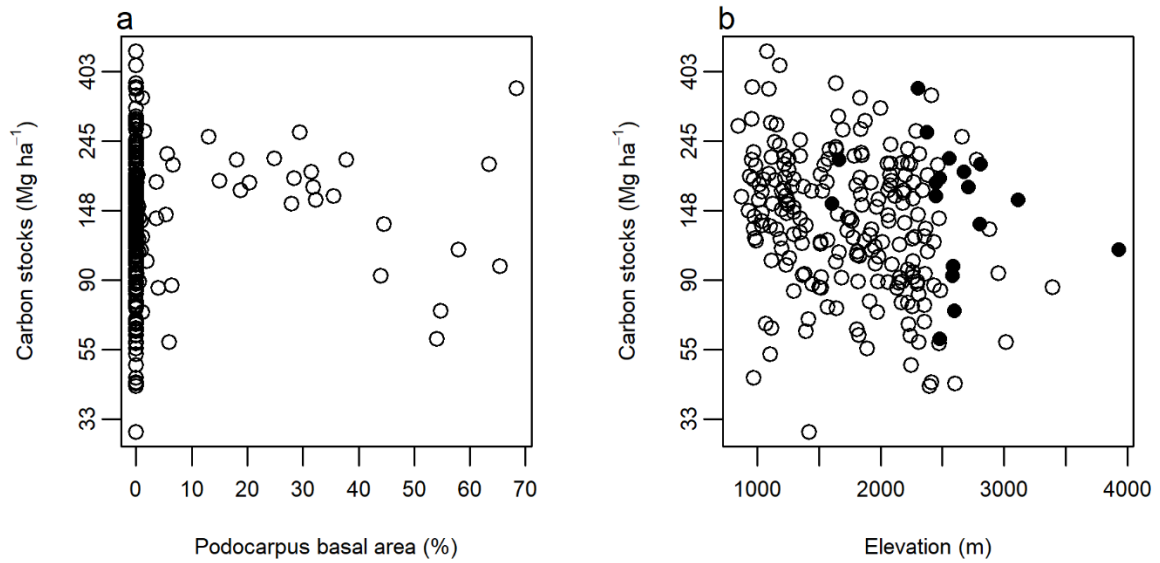
891
 892 **Extended Data Fig. 7 | Differences in the environmental conditions sampled by the AfriMont plot**
 893 **network and the tropical montane forest biome in Africa.** The extent of the biome was defined as
 894 closed-canopy forests $\geq 800\text{m}$ asl in December 2018, extracted from ref.³⁸ and clipped to 'primary
 895 humid forest' using ref.³⁹. Environmental variables for the biome were extracted at $\sim 1\text{-km}$
 896 resolution.

897
 898

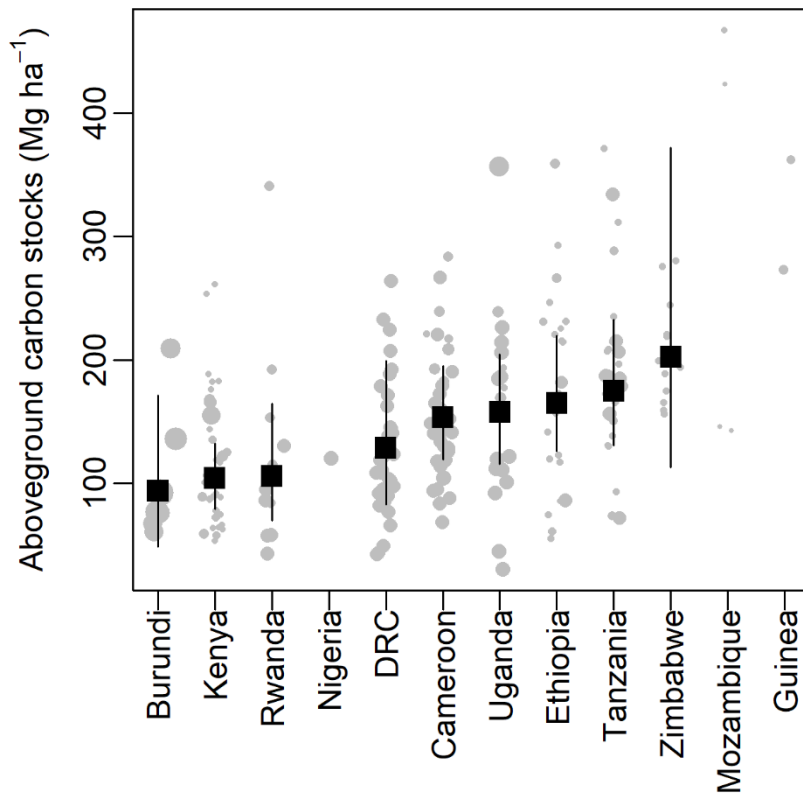


899
 900
 901
 902
 903
 904
 905
 906
 907
 908
 909

Extended Data Fig. 8 | Differences in aboveground carbon (AGC) stocks in AfriMont plots located in montane forests with and without elephants. **a)** Differences across all plots. AGC-stocks are statistically significantly lower in forests with elephants (t -test, $t = 3.5$, $df=83.5$, $P = 0.001$). The thick line shows the median, and boxes cover the interquartile range (IQR). Values > 1.5 times IQR away from the IQR are shown by points. **b)** Differences in countries where elephants are present in at least one of the montane sites studied. Black squares show means in each country in forests with or without elephants – solid lines denote statistically significant differences (t -tests, $P < 0.05$). Elephant presence in 2019 was estimated by co-authors (see Table S5).



910
 911 **Extended Data Fig. 9 | Relationship between aboveground carbon (AGC) stocks and**
 912 **Podocarpaceae.** (a) Relationship between AGC-stocks and Podocarpaceae basal area across plots in
 913 the AfriMont network, expressed as a percentage of total plot basal area. These variables are not
 914 significantly correlated ($r_s = 0.083$, $n = 226$, $P = 0.212$). (b) Distribution of plots with at least 20%
 915 basal area of Podocarpaceae (black points) in relation to elevation and AGC-stocks. AGC-stocks are
 916 not significantly related to elevation or Podocarpaceae basal area (Linear mixed effects model, $P =$
 917 0.152 and 0.132 respectively).
 918
 919



921 **Extended Data Fig. 10 | Within country variation in aboveground carbon stocks based on the**
 922 **AfriMont plot network.** Error bars show means and 95% confidence intervals estimated by linear
 923 mixed-effects models. Modelled means not shown for countries with fewer than five plots. Point size
 924 is proportional to plot area.

925
 926
 927
 928